SERI/TR-9276-T3
(DE82002093)

ELECTROCHEMICAL PHOTOVOLTAIC CELLS/STABILIZATION AND OPTIMIZATION OF II-VI SEMICONDUCTORS

Final Technical Progress Report for April 15, 1980—June 14, 1981

By
Rommel Noufi
Dennis Tench
Les Warren

March 1981

Work Performed Under Contract No. AC02-77CH00178

Rockwell International
Thousand Oaks, California

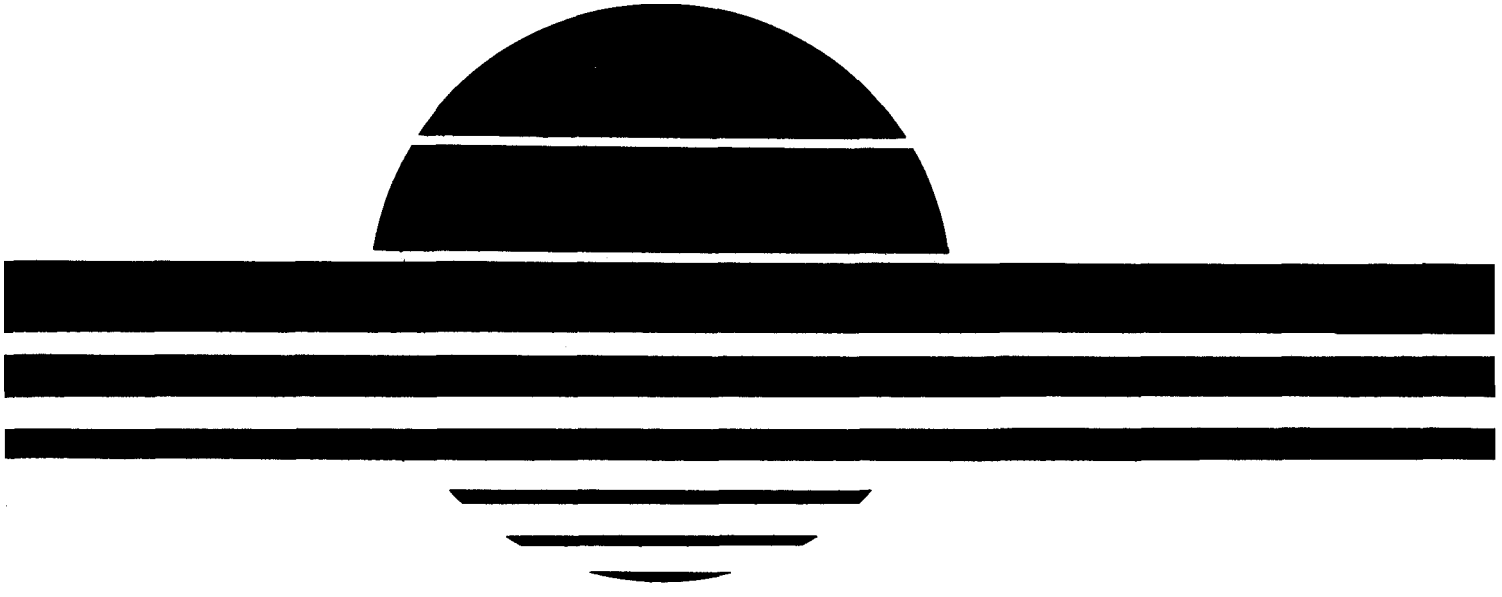

U.S. Department of Energy

Solar Energy

DISCLAIMER

SERI/TR-9276-T3
(DE82002093)
Distribution Category UC-63

FINAL TECHNICAL PROGRESS REPORT

March 1981

Contract Period: 04/15/80 through 06/14/81

Contract Title: Electrochemical Photovoltaic Cells/Stabilization and Optimization of II-VI Semiconductors

Contractor: Rockwell International
Thousand Oaks, California 91360

Authors: Rommel Noufi, Dennis Tench and Les Warren

Contract Number: XG-0-9276

Document Number: ERC41066.28FR

Sponsored By: Department of Energy through the
Solar Energy Research Institute

TABLE OF CONTENTS

LIST OF FIGURES

LIST OF FIGURES (Continued)

LIST OF TABLES

1.0 ABSTRACT

The overall goal of this program is to provide the basis for designing a practical electrochemical solar cell based on the II-VI compound semiconductors. Emphasis is on developing new electrolyte redox systems and electrode surface modifications which will stabilize the II-VI compounds against photodissolution without seriously degrading the long-term solar response.

Factors limiting the short circuit current of the n-CdSe photoanodes in the methanol/ferro-ferricyanide system (which we have shown to be stabilizing) to 17.5 mA/cm^2 were identified. The principal limiting factor is apparently specific adsorption of a ferricyanide species on the electrode surface which occurs at higher redox couple concentrations and slows the overall charge transfer process. Ion pairing also occurs, resulting in a low mass transport rate (smaller diffusion coefficients and increased solution viscosity), and probably enhances the degree of specific adsorption. Although the methanol/ferro-ferricyanide solution itself was found to be photolytically unstable, study of this system led to the identification of more promising nonaqueous redox electrolytes.

Additional work on redox couple stabilization of n-CdX photoanodes was focused on both one- and two-electron couples, including $Fe(EDTA)^{1-/2-}$, $Co(bipy)^{3+/2+}$, $Fe(CN)_4(bipy)^{1-/2-}$, and the chloro-complexes of iron, copper, tin, and antimony in various nonaqueous solvents. Very promising results were obtained for the alkylammonium chloro-Fe(II,III) couple in acetonitrile.

Conducting polymer films of polypyrrole photoelectrochemically deposited onto n-type semiconductors were shown to protect these electrode materials from photodecomposition while permitting electron exchange with the electrolyte, but poor adhesion has remained a key problem. Recently, improved adhesion has been attained for roughened semiconductor surfaces. Good performance characteristics were attained in some cases, although observed dark currents were often appreciable. In a basic aqueous ferro-ferricyanide electrolyte containing cyanide ion, the measured open circuit voltage for n-CdTe was 1.3 V, which is practically the bandgap for this material - a notable result.

It now appears that polypyrrole films are to some extent permeable to solvent/solute species since the film stability depends on the nature of the redox electrolyte, and semiconductor decomposition products seem to form underneath the film in some cases. One possibility for circumventing this problem is to incorporate larger species, e.g., phthalocyanine dyes, within the film matrix. Other conducting polymers may also be used and some work with polyaniline films was performed under the present program. Perhaps, the most promising approach to photoanode stabilization is to utilize conducting polymer films in concert with judiciously chosen stabilizing redox electrolytes.

Work on evaluating photocapacitance spectroscopy as a means of in situ characterization of semiconductor electrodes was focused on developing a reliable measurement technique. With a new computerized system and precautions to avoid stray bandgap light, several distinct peaks were observed in the sub-bandgap photocapacitance spectra for n-GaAs electrodes in aqueous solutions. Considerable additional effort will be required to ascertain whether these peaks arise from optical transitions occurring within the semiconductor, within a surface oxide layer, or at the various interfaces between the semiconductor, electrolyte, and oxide.

2.0 PROJECT DESCRIPTION

To date, the best performance for electrochemical solar cells has been attained with n-type cadmium chalcogenide (CdX, where X = S, Se or Te) [1-15] and n-GaAs [16] electrodes stabilized by chalcogenide/polychalcogenide redox couples (e.g., Se^{2-}/Se_x^{2-}) in aqueous electrolytes. Photogenerated holes, which would otherwise lead to destruction of the semiconductor lattice, are preferentially consumed in the redox reaction. Solar AM2 conversion efficiencies of 7 to 8% for CdX single crystals [10], 6% for thin CdX polycrystalline films [1], and 9% for GaAs single crystals [16] have been reported. Unfortunately, although photodissolution is almost completely suppressed in such systems, the photocurrents deteriorate with time, especially at higher light intensities. In the case of CdX, this has been shown to involve chalcogenide exchange between the electrolyte and the electrode surface, possibly via photo-oxidation followed by reprecipitation [17-20]. Noufi, et al. [1] have demonstrated that conversion efficiencies are higher and degradation is slower for mixed polycrystalline CdS/CdSe electrodes. Chemical modification of n-GaAs electrodes by $RuCl_3$ solutions has also been shown [21] to increase solar conversion efficiencies for single crystals to 12% in Se^{2-}/Se_x^{2-}, although long-term stability has not been established.

These results demonstrate both the promise and the problems associated with stabilization of narrow-band-gap semiconductors for use in electrochemical solar cells. Most studies to date have emphasized cell characterization rather than materials development, so that only the more common semiconductors and a few redox systems have been investigated. In spite of this, decent power conversion efficiencies (6%) for thin polycrystalline films have been demonstrated. To evolve a stable acceptably efficient cell, however, a more systematic approach involving a wider spectrum of materials and more emphasis on materials characterization is needed. The most promising possibilities include organometallic redox systems in both aqueous and nonaqueous media and chemically modified electrode surfaces. Surface chemical modification is particularly attractive since the electrolyte redox system could then be varied over a wider range to improve conversion efficiencies and perhaps obtain more desirable reaction products (e.g., fuels). Unfortunately, the

synthetic chemistry knowledge required for chemically modifying II-VI electrode surfaces is not available and has to be developed.

The program emphasis is on developing new electrolyte redox systems and electrode surface modifications which will stabilize the II-VI compounds against photodissolution without seriously degrading the long-term solar response. A cooperative effort involving electrochemistry, synthetic chemistry, and materials characterization provides the mutual feedback necessary to evolve a practical compromise between the interfacial chemistry and the device characteristics. Work will ultimately concentrate on the polycrystalline thin films needed for large area, economical solar cells, although single crystal electrodes are used to elucidate some of the surface chemistry. Obviously, much of the chemical knowledge required for redox system design and electrode surface modification is similar, so that considerable synergy exists between these two parallel approaches.

A critical facet of this program involves materials characterization. Chemical changes in the electrode surface resulting from deliberate chemical modifications or photoelectrochemical evaluation are detected by x-ray photoelectron spectroscopy (XPS), Auger electron spectroscopy (AES), secondary ion mass spectroscopy (SIMS), energy dispersive analysis of x-rays (EDAX), and/or low energy electron diffraction (LEED). Morphological changes in grain size or porosity are followed by scanning electron microscopy (SEM). Hall, conductivity, and a.c. impedance measurements are used to determine the concentrations, mobilities, and lifetimes of charge carriers in the semiconductor materials. The presence and properties of electrode surface states and trap levels are being investigated *in situ* by photocapacitance spectroscopy, an extremely promising new technique.

This broad interdisciplinary approach permits full advantage to be taken of the synergy which exists between the various facets of the program and of the understanding and insight provided by thorough materials characterization. Actual electrochemical solar cells are also built to test concepts and provide additional feedback for further materials development, as well as a better basis for comparing the emerging electrochemical and solid state solar cell technologies.

3.0 TECHNICAL PROGRESS DESCRIPTION

3.1 Development of New Electrolyte Redox Couples

3.1.1 Methanol/Ferro-Ferricyanide

Under last year's program, n-CdSe photoanodes were shown to be stable in the methanol/ferro-ferricyanide system [22]. Under tungsten-halogen illumination of about AM1 intensity (85 mW/cm^2), the current at a single crystal n-CdSe photoanode remained constant at 6 mA/cm^2 (conversion efficiency of ~ 3.5%) for 29 days in a stirred methanol electrolyte containing 0.4 M each of tetraethylammonium $Fe(CN)_6^{3-/4-}$ plus 0.1 M tetraethylammonium fluoroborate. It was also demonstrated that the stability of n-CdSe photoanodes in methanol/ferro-ferricyanide is not sensitive to traces of water.

Based on these very encouraging results, experiments were then performed using more efficient n-CdSe electrode materials. The best output parameters for n-CdSe (~5.5% conversion efficiency, FF = 0.47) were obtained for electrodes with 5 x 10^{16} carriers/cm^3 in methanolic solutions containing 0.25 M each of chemically prepared $Fe(CN)_6^{3-/4-}$ species. A typical power curve is shown in Fig. 1. The measured open circuit voltage is very close to the maximum value expected for this system (0.7 V). Photocurrent measurements as a function of light intensity indicated that the maximum stable short circuit current is 17.5 mA/cm^2 in stirred solutions and 7.5 mA/cm^2 in unstirred solutions (at 95 mW/cm^2). Transient photocurrents were larger at the higher light intensities but rapidly decayed to the steady values. Currents of 17.5 mA/cm^2 were passed for as long as 2 hours.

Under the current program, the factors limiting the attainable photocurrent in the n-CdSe/methanol/ferro-ferricyanide system were determined. The possibilities included inadequate mass transport of the redox species in the electrolyte and decreased redox reaction rate caused by ion pairing or specific adsorption of one or both of the electroactive species. The inherent electrode kinetics for the ferro-ferricyanide couple in methanol were studied by cyclic voltammetry at a rotating Pt disc electrode. Kinematic viscosity measurements were also made as a function of the redox couple concentration so

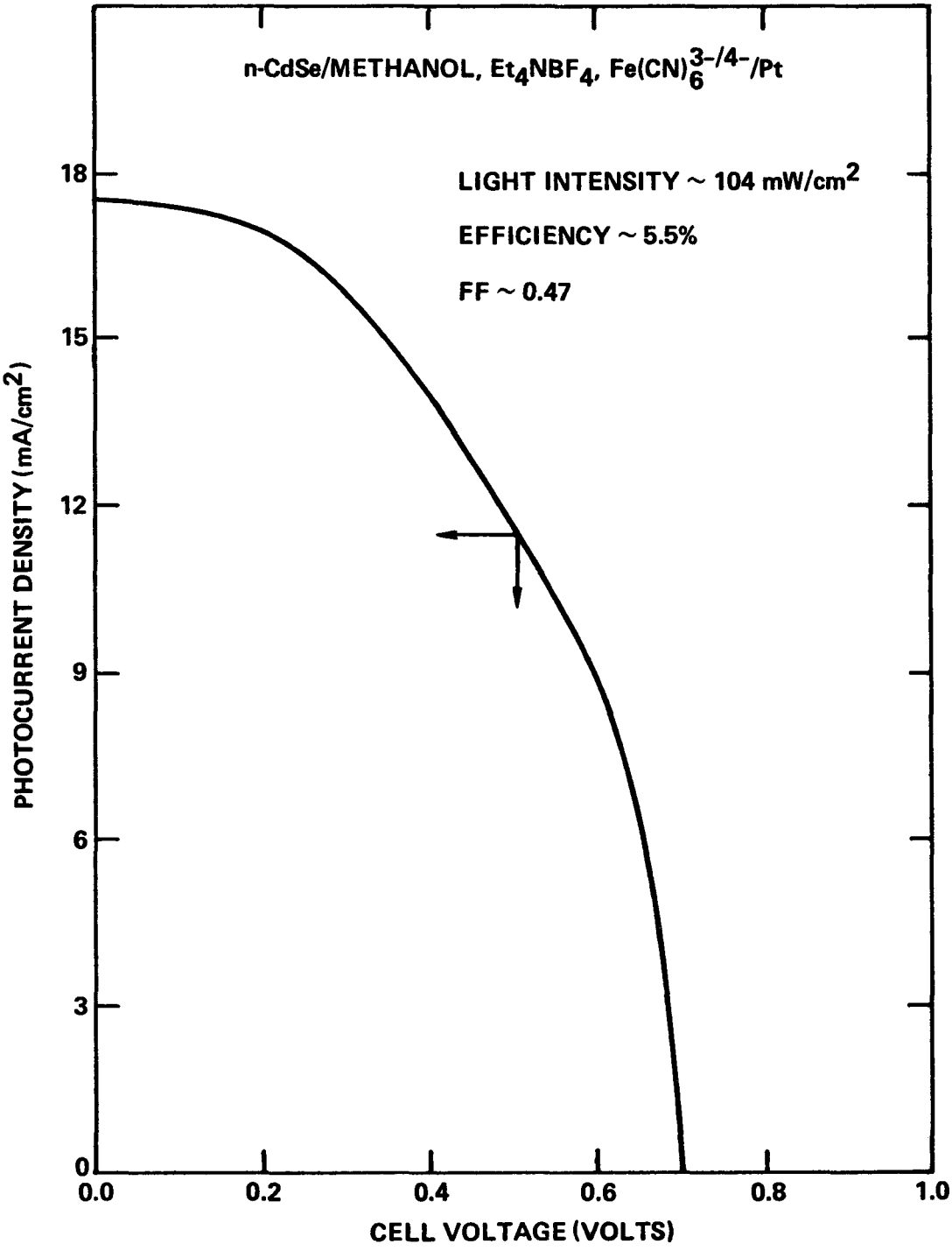

Fig. 1 Photocurrent density vs voltage for the cell n-CdSe/methanol, 0.25 M $Fe(CN)_6^{3-/4-}$, 0.1 M Et_4NBF_4/Pt under illumination at 104 mW/cm^2.

that the relative effects of changes in the fluid flow characteristics, reactant diffusion coefficients, and electron transfer rate could be ascertained. The dependence of the photocurrent for n-CdSe photoanodes on light intensity was determined in both the methanol/ferro-ferricyanide and aqueous polysulfide systems as a means of detecting solid state limitations. Some earlier measurements were repeated as a check.

Figure 2 shows plots of the diffusion-limited currents (i_L) for the ferro-ferricyanide reaction at a rotating Pt disc electrode as a function of the redox couple concentration. For both the anodic and cathodic branches, i_L goes through a maximum at about 0.15 M $Fe(CN)_6^{3-/4-}$. Also, at concentrations above 0.05 M, specific adsorption becomes significant as indicated by higher "Tafel" slopes (180-250 mV/decade) than obtained at lower concentrations (~120 mV/decade). The decrease in i_L at higher concentrations could result from a decrease in the diffusion coefficient of the hexacyanoferrate species, stemming from increased ion pairing, and/or an increase in the electrolyte viscosity. That i_L is practically diffusion-limited at all redox couple concentrations is shown by the Levich plots [23] in Fig. 3.

Figure 4 shows plots of the diffusion coefficients for the $Fe(CN)_6^{3-/4-}$ species (calculated from the Levich equation) and the electrolyte kinematic viscosity (measured with a Cannon-Fenske viscometer) vs the redox couple concentration. The viscosity is practically constant at low $Fe(CN)_6^{3-/4-}$ concentrations but increases sharply at about 0.2 M, which corresponds approximately to the maximum in the diffusion-limited current for the redox reaction (0.15 M). However, the diffusion coefficient decreases by almost an order of magnitude (from 28×10^{-6} to 3×10^{-6} cm^2/sec) from 0.01 to 0.1 M $Fe(CN)_6^{3-/4-}$, indicating that considerable ion pairing occurs even at relatively low redox couple concentrations. Ion pairing of hexacyanoferrate species with tetraalkylammonium cations in solvents with low acceptor numbers has also been detected polarographically [24].

The relative effects of the electrolyte kinematic viscosity (ν) and the diffusion coefficients (D) in reducing the diffusion limiting currents can best be seen by plotting $D^{2/3}$ and $\nu^{-1/6}$, which are the terms appearing in the Levich equation [23].

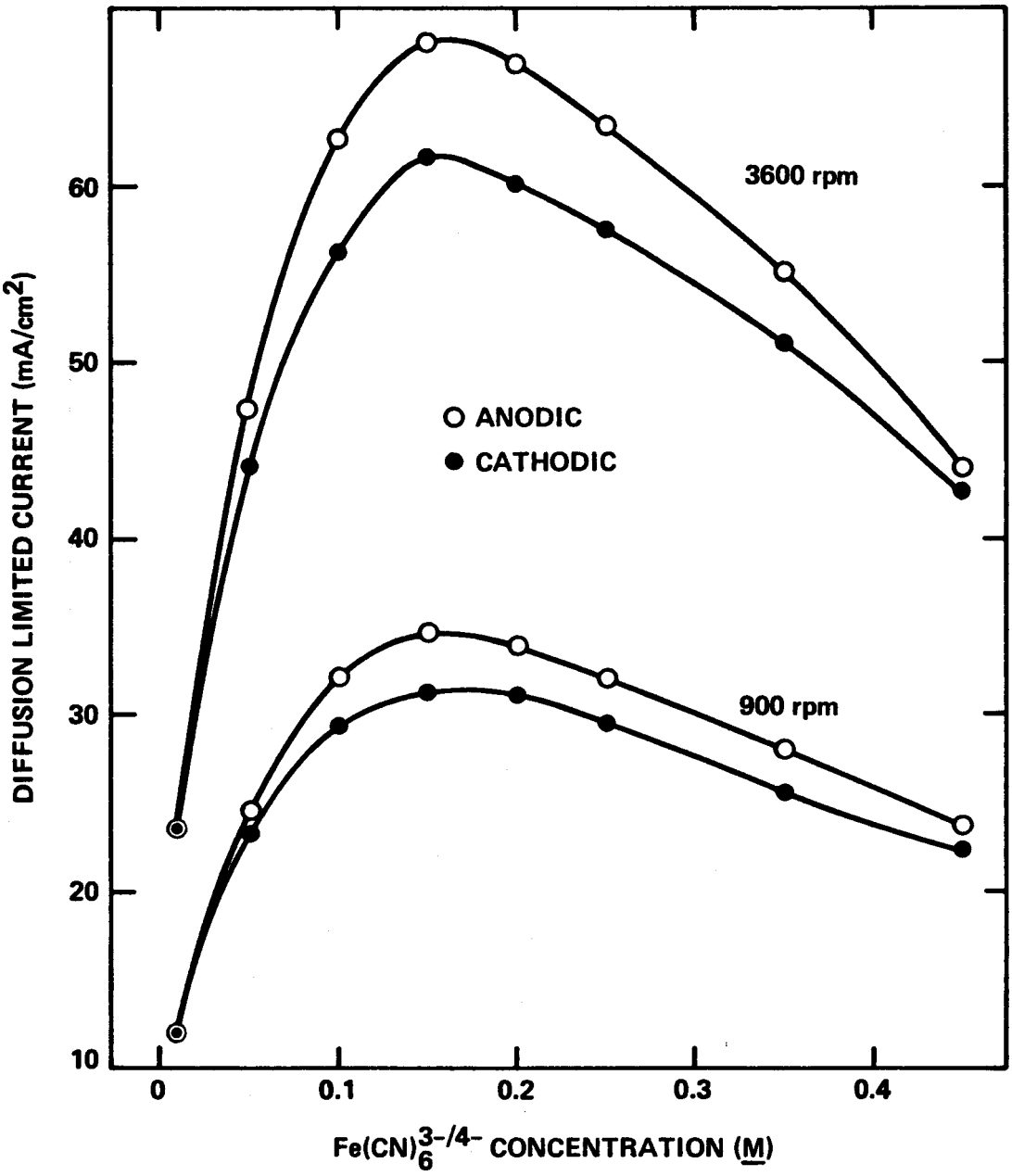

Fig. 2 Diffusion-limited currents vs the $Fe(CN)_6^{3-/4-}$ concentration for a rotating 0.13 cm^2 Pt disc electrode in methanol/0.1 M Et_4NBF_4 electrolyte containing equal concentrations of the oxidized and reduced species. The scan rate was 20 mV/sec and i_L was determined at an overvoltage of 1.00 V in each case.

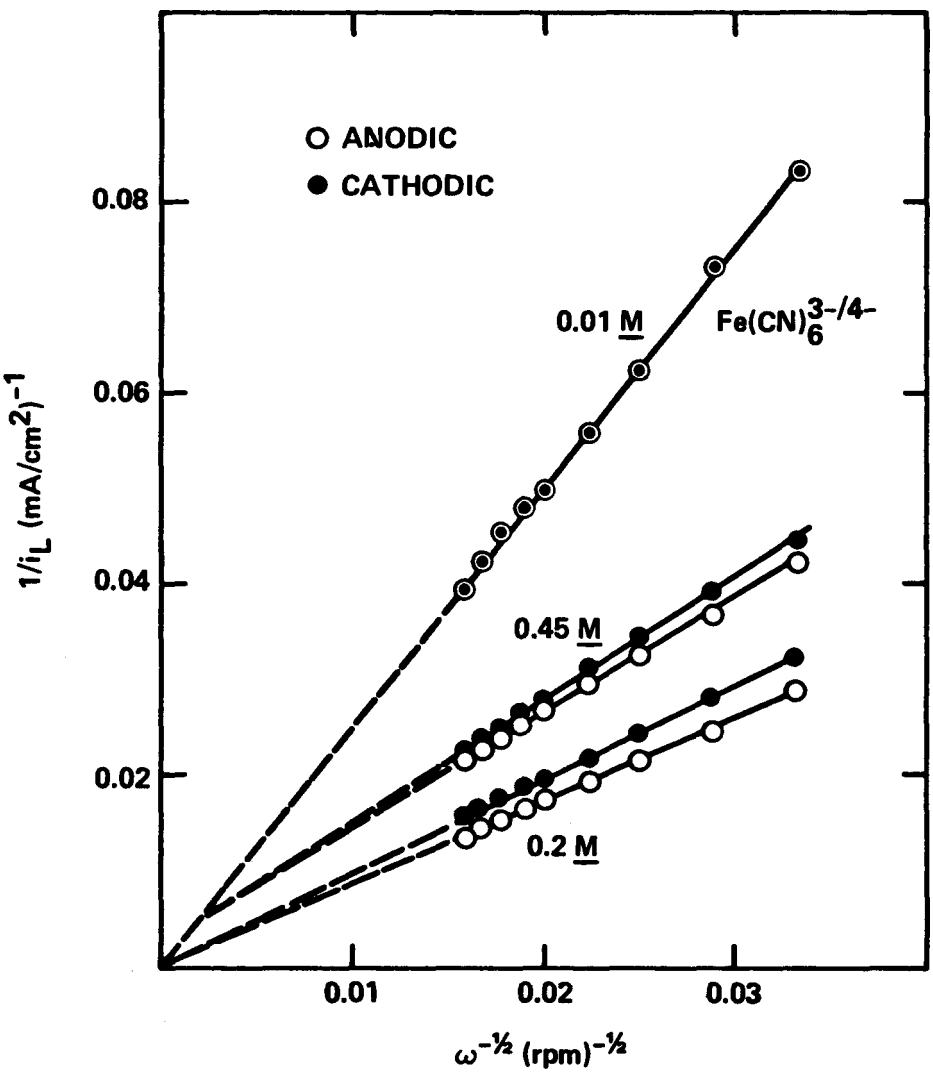

Fig. 3 Levich plots [23] for the $Fe(CN)_6^{3-/4-}$ reaction at a rotating Pt disc electrode in methanol/0.1 M Et_4NBF_4 (conditions same as for Fig. 2).

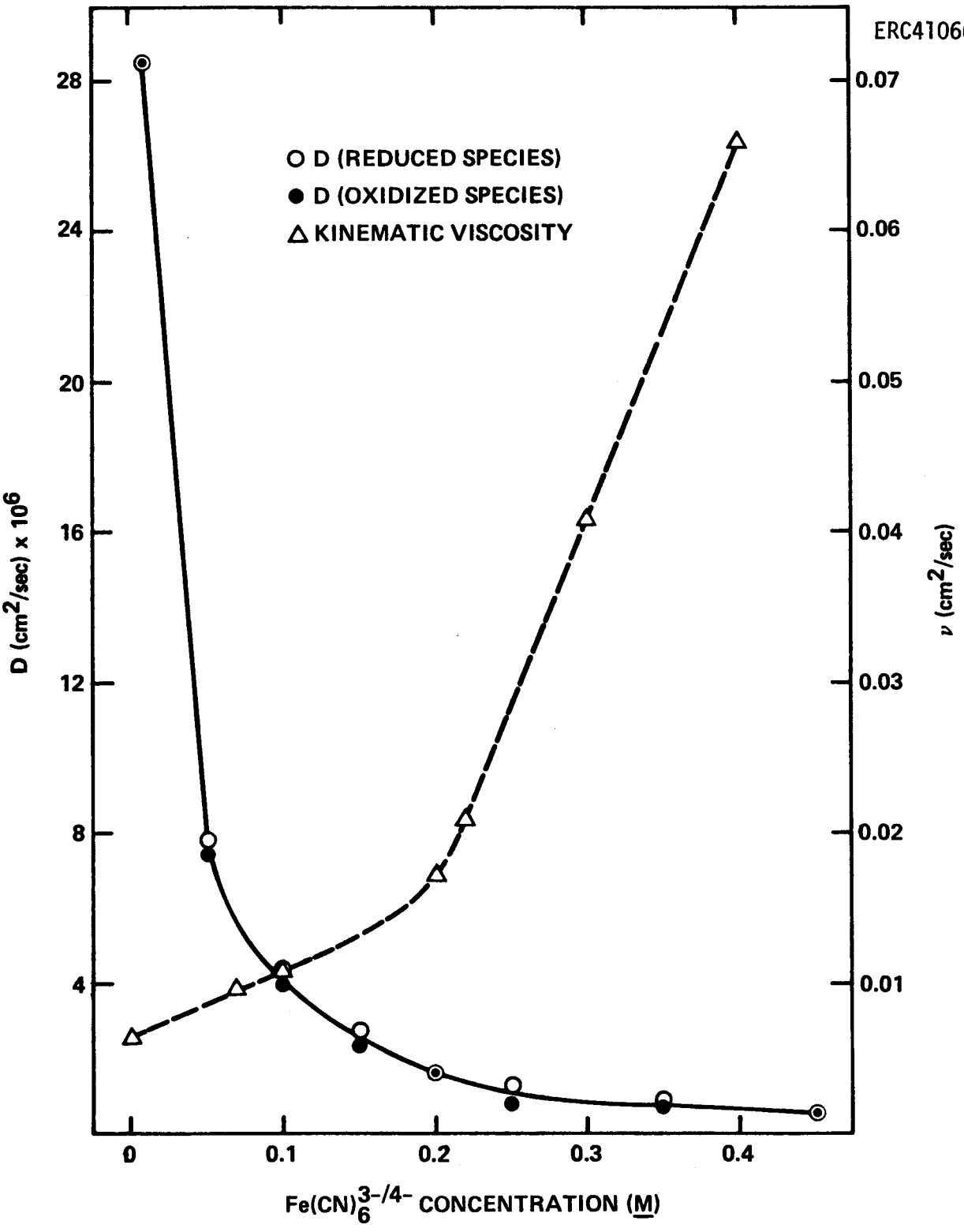

Fig. 4 Plots of the diffusion coefficients (D) of $Fe(CN)_6^{3-/4-}$ species and the kinematic viscosity of 0.1 M Et_4NBF_4/methanol solutions as functions of the $Fe(CN)_6^{3-/4-}$ concentration.

$$i_L = 1.94 \times 10^7 \, C_R \, D_R^{2/3} \, \nu^{-1/6} \, \omega^{1/2}$$

where i_L is in mA/cm^2, C_R is the concentration of reactant in moles/ml, D_R is the reactant diffusion coefficient in cm^2/sec, ν is the electrolyte kinematic viscosity in cm^2/sec, and ω is the disc electrode rotation rate in rpm. Such plots are shown in Fig. 5, where $\nu^{-1/6}$ is seen to decrease linearily and relatively slowly (note scale difference) with $Fe(CN)_6^{3-/4-}$ concentration, whereas, $D^{2/3}$ decreases sharply to about 0.1 M and then more gradually. Thus, the decrease in i_L at concentrations above 0.15 M results from a combination of the effects of $\nu^{-1/6}$ and $D^{2/3}$.

Plots of the short-circuit photocurrent at single crystal n-CdSe photoanodes in 0.25 M $Fe(CN)_6^{3-/4-}$/methanol and in aqueous polysulfide electrolytes vs light intensity are shown in Fig. 6. The linear plot (passing through the origin) for the aqueous system indicates that solid state limitations are not predominant. Therefore, the nonlinearity in the methanol/$Fe(CN)_6^{3-/4-}$ plot and the upper limit of 17.5 mA/cm^2 for the steady-state photocurrent are apparently associated with electrolyte effects. The data can be adequately explained by assuming the occurrence of strong specific adsorption of a ferricyanide species, which is the product of the photoelectrochemical redox reaction. Thus, at the lower light intensities, for which the currents are lower, the reaction rate is under mixed electron transfer/product desorption control, i.e., the rates of electron transfer (which is determined by the availablity of photoholes in the semiconductor) and product desorption are comparable. As the light intensity (and consequently the current) is increased, the electron transfer rate increases and product desorption becomes the slow reaction step. In this case, higher currents can be passed for a short time but product accumulation on the electrode surface ultimately limits the current to a constant value determined by the rate of desorption. This model is consistent with the transient photocurrents (at the higher light intensities) decaying to the steady state value (Fig. 6), and with the higher Tafel slopes (on Pt) for higher redox couple concentrations. The adsorbed species may be either the ferricyanide species normally present in solution or some reaction intermediate, and it may be ion-paired since the viscosity data

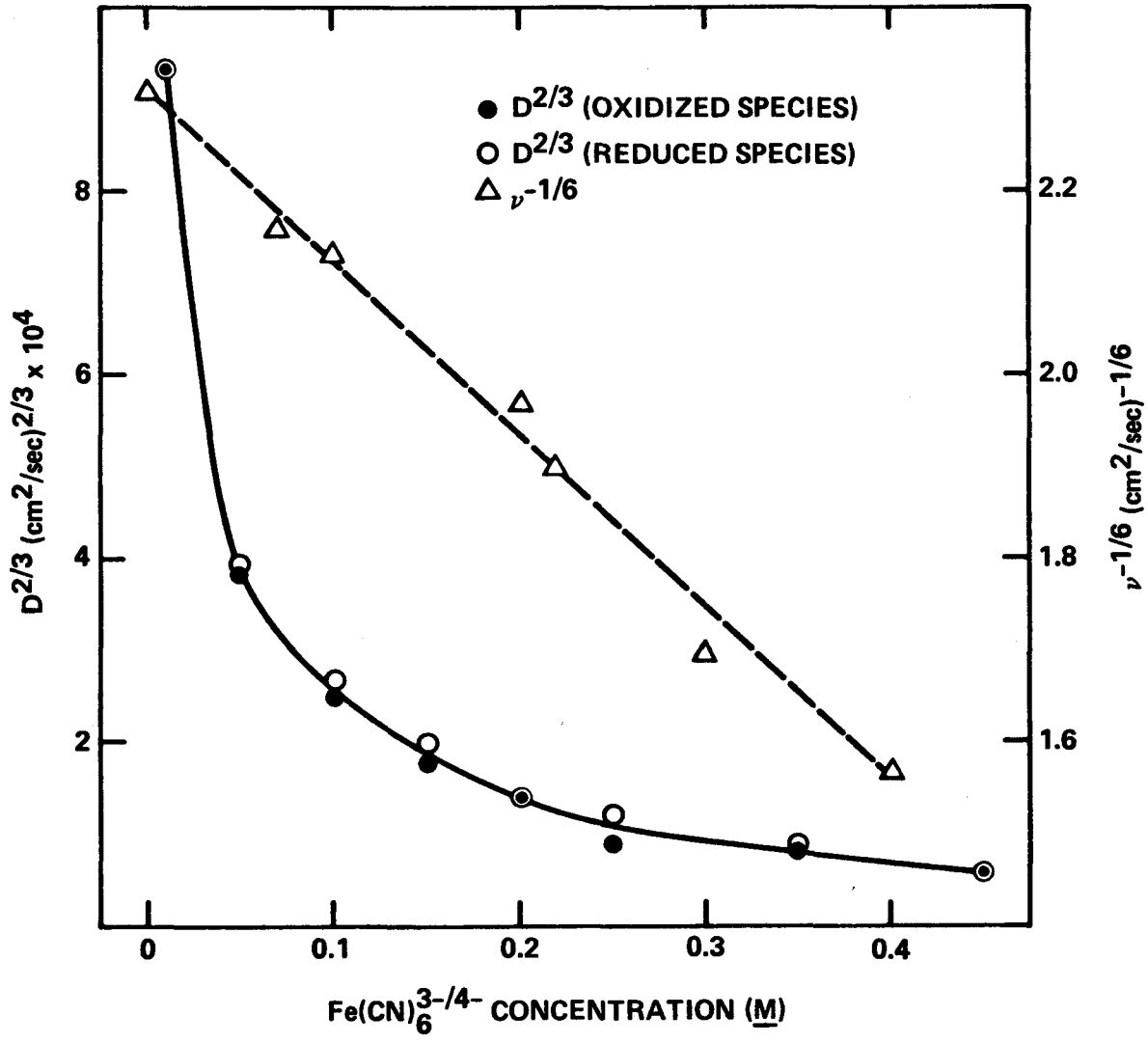

Fig. 5 Plots of $D^{2/3}$ and $\nu^{-1/6}$ for the data in Fig. 4.

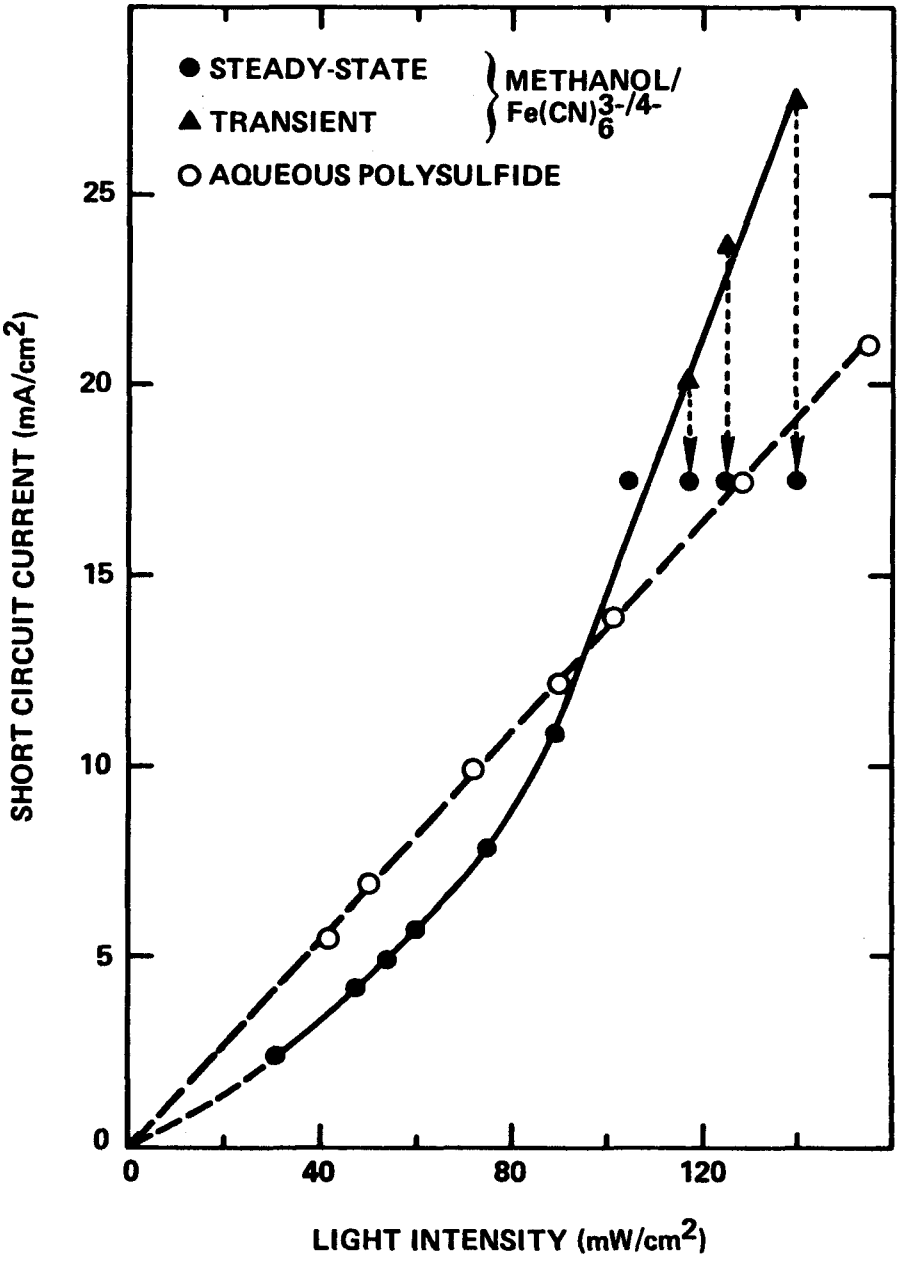

Fig. 6 Short-circuit currents vs light intensity (tungsten-halogen lamp) for n-CdSe electrodes in 0.25 M tetraethylammonium $Fe(CN)_6^{3-/4-}$/0.1 M Et_4NBF_4/methanol and in aqueous 2.2 M Na_2S/0.1 M S/0.1 M NaOH electrolytes.

indicate that ion pairing is prevalent at $Fe(CN)_6^{3-/4-}$ concentrations above 0.1 M. Note that specific adsorption is known to also occur for the aqueous polysulfide system but would not affect the linearity of the corresponding plot in Fig. 6 if adsorption/desorption is fast compared to the electron transfer step, which involves two electrons.

Ultimately, solutions of the $Fe(CN)_6^{3-/4-}$ couple in methanol were found to turn slowly from yellow to orange in the sunlight. This color change, while much slower than in water, was also observed with solutions stored in the drybox under fluorescent light and is strongly indicative of partial cyanide photosubstitution in the hexacyanoiron molecule to form colored (red to purple) pentacyano-iron-ligand derivatives. The associated release of free cyanide ion by such substitution reactions and darkening of the solution are expected to be detrimental to the long-term performance of PEC's utilizing these compounds. We presently know of no effective way to quench the photo-reactions in this system other than to block out those wavelengths responsible, an unrewarding proposition. Consequently, the methanol/$Fe(CN)_6^{3-/4-}$ system was not investigated further.

3.1.2 Other Redox Electrolytes

Although the methanol/$Fe(CN)_6^{3-/4-}$ system does not appear to be practical for photoanode stabilization, our studies with this system demonstrated the efficacy of fast one-electron redox couples in stabilizing n-CdSe electrodes towards photodecomposition in non-aqueous media under AM1 illumination, and pointed the way for further work. Proceeding with this concept, we examined a number of related redox systems, considering only couples expected to be relatively transparent since we feel that good efficiencies will require frontside illumination. The couples investigated include: $Fe(EDTA)^{1-/2-}$, $Co(2,2'\text{-bipyridyl})_3^{3+/2+}$, $Fe(CN)_4(2,2'\text{-bipy})^{1-/2-}$, and chloro complexes of iron, copper, tin, and antimony in various nonaqueous solvents.

Fe(EDTA)$^{1-/2-}$ in Methanol. These iron redox species are soluble in methanol as the triethylammonium salts, which were prepared by treating a slurry of dry $Fe^{II}(EDTAH_2)$ and $Fe^{III}(EDTAH)$ in methanol with just enough

triethylamine to dissolve all the solids. (The latter iron compounds were made from Fe° and $EDTAH_4$ in boiling water, and from $Fe(OH)_3$ and $EDTAH_4$ in water at room temperature, respectively.) The redox solutions ($E° \sim +0.05$ V vs SCE) were brown and exhibited excessive dark currents, small open circuit voltages, and poor fill factors with n-CdX electrodes. This couple was consequently abandoned.

$Co(bipy)_3^{3+/2+}$ in Acetonitrile. Members of this couple were isolated as their perchlorate salts by established procedures [25]. The oxidized species was only soluble in acetonitrile to about 20 mM. The acetonitrile electrolyte containing both couple members was brown and yielded an $E° \sim +0.35$ V on Pt. With CdX electrodes, large dark currents, very small V_{oc}'s, and poor fill factors were observed. This couple was not considered further.

$Fe(CN)_4(bipy)^{1-/2-}$. $K_2Fe(CN)_4(bipy)$ and $HFe(CN)_4(bipy)$ were prepared by the published methods [26]. In water at pH 7, the red ferro-ferricyanide analog displayed an $E° \sim +0.34$ V on Pt and, not unexpectedly, failed to stabilize n-CdSe against photodecomposition. In methanol, ($E° \sim +0.22$ V), the Fe^{II} member was intense violet, and the Fe^{III} species irreversibly oxidized the solvent. In other organic solvents, the intense purple to green colors of the couple precluded further consideration.

3.1.3 Nonaqueous/Chloro-Metal Complexes

More promising results were obtained with chloro-metal couples, e.g., chloro-iron(II,III) and chloro-antimony(III-V), in acetonitrile solutions. These couples are readily prepared (unlike the nonaqueous ferro-ferricyanide couple) and are particularly amenable to modifications which may favorably alter their electron-transfer kinetics to reduce dark currents or improve photoanode stability. Variations of the solvent, chloride ion content, and the size and substituents of the cations were considered. The lower negative charges on the chloro species relative to the ferro-ferricyanide anions suggest that specific adsorption and mass transport limitations due to ion-pairing may not be as severe. Also, these chloro-couples are reasonably transparent, a feature which is seldom found for redox couples in nonaqueous

solvents. The long term photochemical stabilities of the chloro-complexes are also expected to be good.

$FeCl_4^{1-/2-}$. The tetrachloro complexes of iron(II,III) were initially isolated as their tetraethylammonium (Et_4N) salts [27]. In methanol, (E° ~ +0.32 V on Pt), the yellow solution was not stabilizing towards n-CdSe. However, in stirred acetonitrile solution containing 0.12 M $(Et_4N)_2FeCl_4$ and 0.03 M $(Et_4N)FeCl_4$ with 0.1 M TBAP (E° = 0.00 V) , n-CdS and n-CdSe photoanodes yielded open circuit voltages of about 700 mV and were at least partially stabilized. For single crystal n-CdS, the short circuit photocurrent of 2 ma/cm^2 remained stable after passage of charge corresponding to 2X the weight of the crystal. Note that higher photocurrents are difficult to obtain for CdS because the yellow couple absorbs an appreciable fraction of the useable light for this material. Preliminary studies indicate that n-CdSe is about 90% stabilized in the chloro-iron/acetonitrile electrolyte, based on weight loss of the crystal after passage of 140 coulombs at 2 ma/cm^2. n-CdTe appeared to be unstable in this system, whereas GaAs photoanodes were apparently stable. Note that the solubilities of the Et_4N^+ salts in acetonitrile precluded use of redox couple concentrations higher than 0.12 M for Fe^{II} or 0.03 M Fe^{III}.

Studies were performed with higher concentrations of the chloro-iron complexes in acetonitrile by utilizing the more soluble benzyltriethylammonium ($BzBt_3N^+$) salts, in which a benzyl ($-CH_2Ph$) group is substituted for an ethyl group in the Et_4N^+ cations. These complexes were isolated in the same manner as the Et_4N^+ salts with $BzEt_3N^+Cl^-$, dried in vacuo, and examined in an inert atmosphere in dry acetonitrile (distilled from P_2O_5). Unlike the nonaqueous ferri-ferrocyanide system, viscosity effects do not appear to be a problem with the $BzEt_3N^+FeCl_4^{1-/2-}$ couple at the higher (>0.1 M) concentrations in acetonitrile. The output parameters and stability of n-CdSe photoanodes were determined as a function of the chloride content of the solution. In the "neutral" $4Cl^-$/Fe case (0.2 M $FeCl_4^{2-}$, 0.05 M $FeCl_4^-$, 0.1 M $TBAPF_6$), V_{oc} = 0.68 V and n-CdSe is partially stabilized at a short-circuit current density >2 mA/cm^2, but at higher currents, a red Se$^\circ$ layer forms at the semiconductor surface within a short period of time. In a "basic" solution

containing more than four Cl^- per Fe atom (0.2 M $FeCl_4^{2-}$, 0.05 M $FeCl_4^-$, 0.1 M Cl^-), little change was observed in the solution color or V_{oc}; however, the stability of the CdSe photoanode was noticeably reduced relative to the "neutral" electrolyte. Consequently, the presence of free chloride ion is apparently detrimental to the photostability of n-CdSe in acetonitrile. In going to an "acidic" electrolyte with less than 4 Cl^-/Fe, i.e., 0.2 M $FeCl_4^{2-}$, 0.05 M $FeCl_4^-$, 0.1 M $TBAPF_6$, and 0.1 M anhydrous $FeCl_2$ (a Lewis acid prepared by heating pure $FeCl_2 \cdot 4H_2O$ in vacuo), the single reversible one-electron wave on Pt separated into two overlapping waves and the V_{oc} dropped to 0.40 V. In effect, the lower chloride ion content resulted in an increase in the dark reduction current at the semiconductor electrode with this fast one-electron couple. Photoanode stability was comparable to that in the "neutral" electrolyte and the solution darkened to an orange color. Figure 7 illustrates the effect of Cl^- on the $FeCl_4^{1-/2-}$/acetonitrile couple.

Since the coordinated Cl^- ions in $FeCl_4^{1-/2-}$ are readily displaced by the solvent in methanol solutions and free chloride apparently assists the photodecomposition of CdX photoanodes, improved stability might be attained in this case by employing a free chloride scavenger, such as anhydrous $CdCl_2$ (a Lewis acid). Our preliminary results tend to substantiate this assumption, at least for n-CdS. For these studies, the electrolyte contained unpurified "anhydrous" $FeCl_2$, $FeCl_3$, and $CdCl_2$ (which was intended to scavenge any free chloride ions as $CdCl_3^-/CdCl_4^{2-}$ anions). This yellow redox couple exhibits an E° of ~0.44 V and, for n-CdS, $V_{oc} \cong 0.75$ V. By analogy with the $Fe(CN)_6^{3-/4-}$ couple, which is partially stabilizing to CdX photoanodes in aqueous electrolytes and totally stabilizing in methanol solutions, the $Fe^{3+/2+}$ couple,*

*In nonaqueous media, $Fe^{3+/2+}$ refers to the chloro species, i.e., $FeCl^{2+/1+}$ $FeCl_2^{1+/0}$, and $FeCl_3^{0/1-}$, where the remaining coordination sites are occupied by solvent molecules. Voltammograms on Pt in acetonitrile solution show distinct waves corresponding to these couples. The non-chloride containing species, $Fe(solvent)_n^{3+/2+}$, are very difficult to obtain in anhydrous form and, at least in acetonitrile, are very strongly oxidizing.

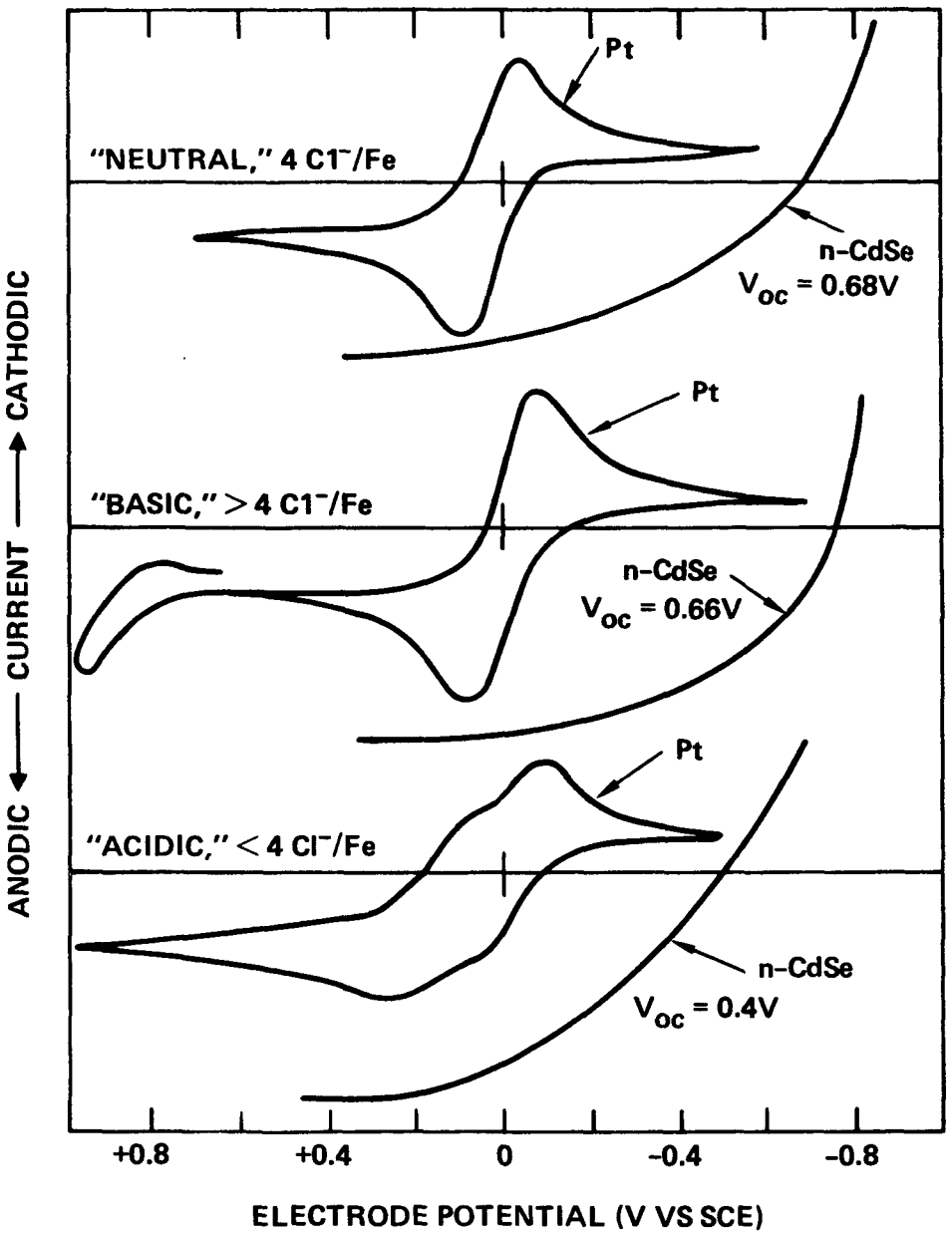

Fig. 7 Cyclic voltammograms at 100 mV/sec for n-CdSe and Pt electrodes in a "neutral" acetonitrile solution containing 0.2 M $FeCl_4^{2-}$ + 0.05 M $FeCl_4^-$ (as $BzEt_3N^+$ salts) + 0.1 M $TBAPF_6$, a "basic" electrolyte with 0.1 M Cl^- as the supporting electrolyte (instead of $TBAPF_6$), and an "acidic" electrolyte made by adding 0.1 M anhydrous $FeCl_2$ to the "neutral" system.

which is partially stabilizing in aqueous media, may also prove to be totally stabilizing in methanol or acetonitrile.

Chloro-Copper(I,II). CuCl and $CuCl_2$ dissolve in methanol or acetonitrile containing excess tetraethylammonium chloride to form colorless copper(I) ($CuCl_2^-$, $CuCl_3^{2-}$, $CuCl_4^{3-}$) and brown to orange copper(II) ($CuCl_4^{2-}$) species. The E° values vary depending on the solvent and the amount of Cl^- added. For example, in methanol solutions containing 3 moles of Cl^- per mole of Cu(I) and Cu(II), E° ~ +0.37 V, whereas in acetonitrile, E° ~ +0.60 V. As in the case of the iron-chloro complexes, only the aprotic solvent acetonitrile afforded reasonable photoanode (n-CdSe) output parameters with the chloro-copper couple.

Addition of three equivalents of chloride ion (as Et_4NCl) to the dark brown acetonitrile solution of the anhydrous halides (0.1 M each) turned the solution orange. This conversion was investigated by cyclic voltammetry on Pt and was shown to involve two separate redox couples: brown $CuCl_2(ACN)_2^{0/-1}$ (E° ~ +0.40 V) and orange-yellow $CuCl_4^{2-/3-}$ (E° ~ +0.07 V). The latter couple, which is preferred because of its lighter color, displayed a broadened wave (unlike the corresponding reversible $FeCl_4^{1-/2-}$ couple), and the presence of free Cl^- ion, which can be detrimental to the stability of photoanodes, was indicated. This is due to the lability of the tetrachloro-copper(I) species, $CuCl_4^{3-}$, in this solvent.

$$CuCl_4^{3-} \rightleftarrows CuCl_3^{2-} + Cl^- \rightleftarrows CuCl_2^- + 2Cl^-$$

The performance of this couple in stabilizing CdS and CdSe photoanodes was poor and dark currents were excessive.

Chloro-Antimony(III,V) and -Tin(II,IV). The encouraging results obtained with the $FeCl_4^{1-/2-}$ in acetonitrile prompted us to consider related metal-based chloro-complexes, in particular, the essentially colorless two-electron systems involving tin and antimony:

$$SnCl_3^- + 3Cl^- \rightleftarrows SnCl_6^{2-} + 2e^-$$

$$SbCl_4^- + 2Cl^- \rightleftarrows SbCl_6^- + 2e^-$$

Dark currents were expected to be smaller with these two electron couples relative to the one-electron systems. Although reduction of the oxidized members in this case releases free chloride ion, it was hoped that its concentration in the electrolyte could be suppressed by a Cl^- scavenger, e.g., $SbCl_3$ or $SnCl_4$.

The antimony(III,V) couple has received the most attention thus far. Benzyltriethylammonium salts of $SbCl_4^-$ and $SbCl_6^-$ were prepared from $BzEt_3N^+Cl^-$ with $SbCl_3$ and $SbCl_5$ in concentrated hydrochloric acid. The resulting air-stable crystalline precipitates were washed with acid and dried in vacuo. The "neutral" acetonitrile solution containing 0.2 M each $SbCl_4^-$ and $SbCl_6^-$, and 0.1 M $TBAPF_6$ is pale yellow and displays a highly irreversible redox wave on Pt with an $E^\circ \sim +0.50$ V, as shown in Fig. 8. Peaks corresponding to oxidation of Sb(III) and reduction of Sb(V) occur at +1.0 and +0.1 V, respectively. On the second voltage scan, following the reduction, a chloride oxidation wave is observed at +0.75 V, indicating that Cl^- is released during the reduction process. In this electrolyte, CdSe rapidly formed an orange surface layer, whereas, CdS appeared to be stable (~12 h, at 0.7 mA/cm^2) and exhibited an open circuit voltage of 0.87 V. However, the photodecomposition products may have dissolved in the electrolyte since the electrode surface was clearly etched.

The effect of chloride ion on the behavior of the n-CdS/Sb(III,V)/acetonitrile system was also examined. Addition of 0.1 M Cl^- to the 0.2 M $SbCl_4^-$, 0.05 M $SbCl_6^-$, 0.1 M $TBAPF_6$ solution turned the solution from pale yellow to orange. Some salting out of $BzEt_3N^+SbCl_4^-$ also occurred. Chloride ion oxidation on Pt was evident at +0.78 V, cathodic of Sb(III) oxidation (+1.03 V). The excess chloride increased the open circuit voltage by 50 mV to 0.92 V, and the fill factor slightly. Performance characteristics for this system are illustrated in Fig. 9.

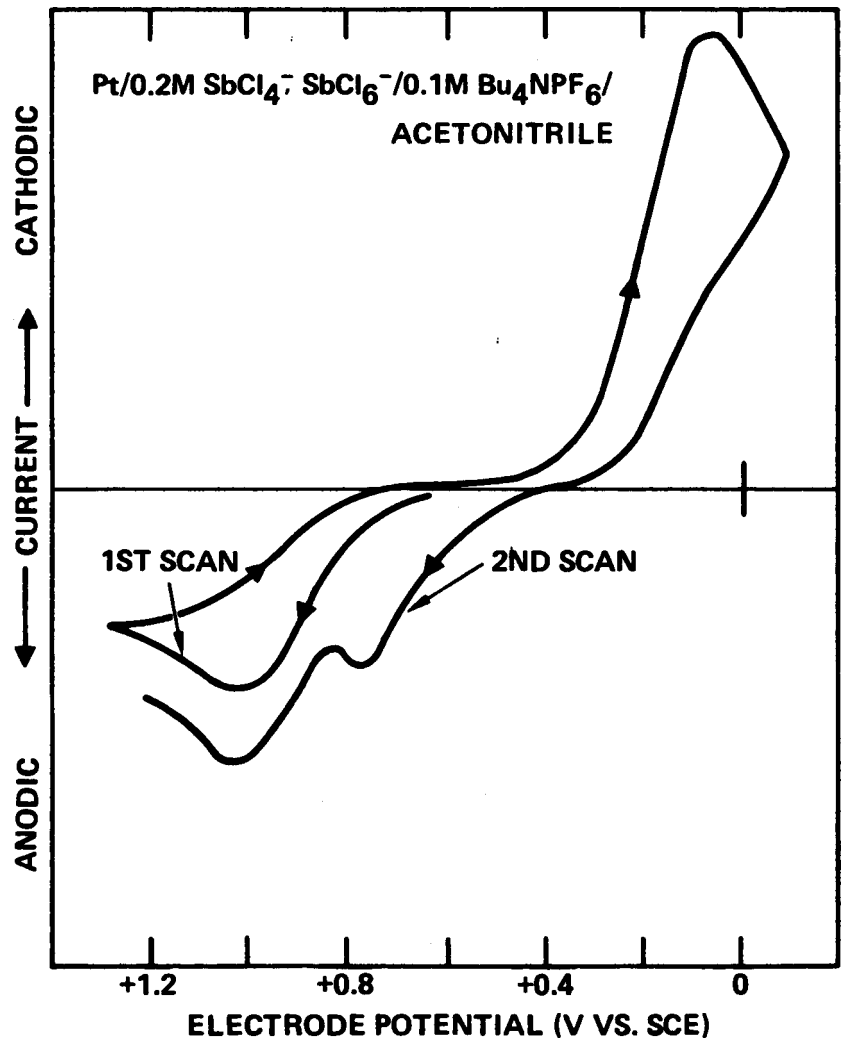

Fig. 8 Cyclic voltammograms at 100 mV/sec for a Pt electrode in acetonitrile solution containing 0.2 M each $SbCl_4^-$ and $SbCl_6^-$ + 0.1 M $TBAPF_6$.

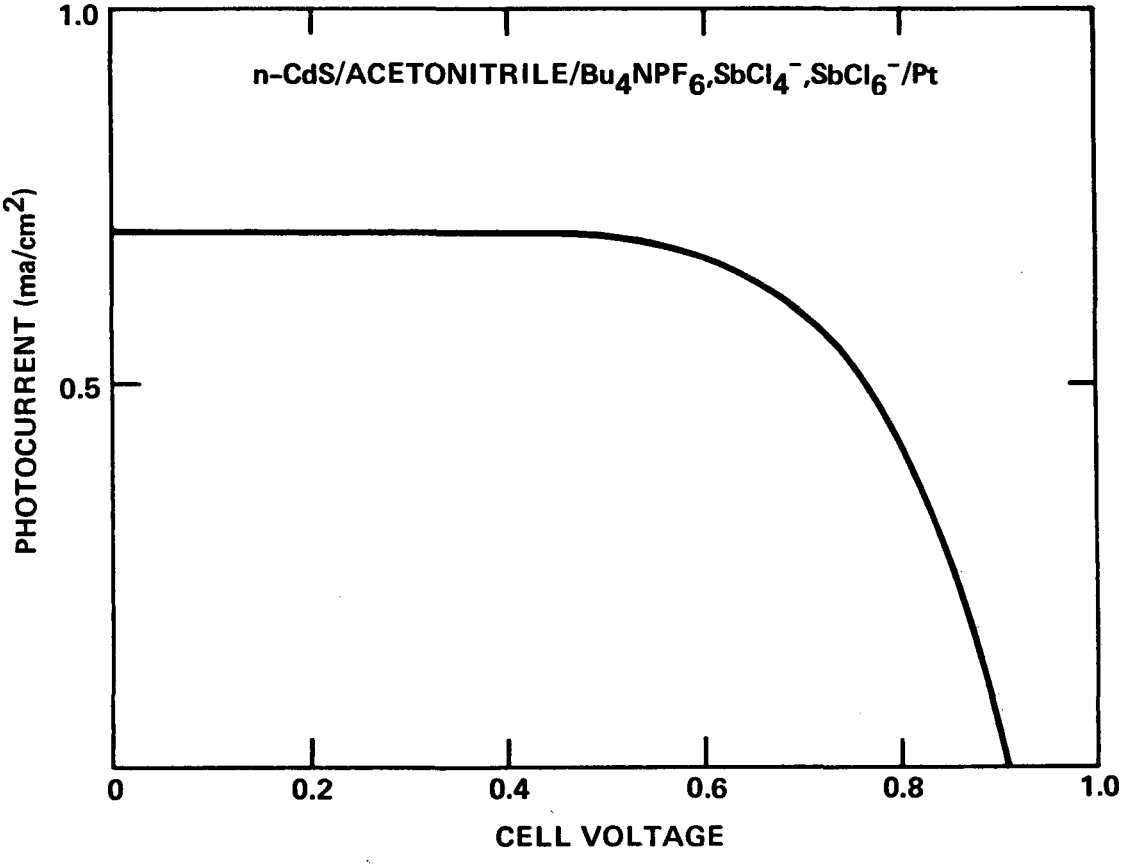

Fig. 9 Photocurrent density vs voltage for the cell n-CdS/acetonitrile, 0.2 M each $SbCl_4^-$ and $SbCl_6^-$, 0.1 M Cl^- (all as $BzEt_3N^+$ salts), 0.1 M $TBAPF_6$/Pt.

In an "acidic" electrolyte containing 0.2 M $SbCl_4^-$, 0.07 M $SbCl_6^-$, 0.1 M $TBAPF_6$, and 0.07 M $SbCl_3$, no free Cl^- oxidation was observed on the reverse scan on Pt following reduction of Sb(V). Thus, the Lewis acid $SbCl_3$ apparently acts as a chloride ion scavenger. The color of the solution remained pale yellow and the E° increased slightly to ~ +0.6 V. The open circuit voltage with n-CdS was essentially unchanged from that for "neutral" electrolyte (0.90 V), although the fill factor was slightly reduced. This behavior is quite different from that of the "acidic" $FeCl_4^{1-/2-}$ couple in acetonitrile, for which the solution color darkened and a substantially reduced V_{oc} was observed upon addition of the Lewis acid $FeCl_2$. With the slower two-electron antimony(III,V) system, dark reduction currents apparently are not as severe a problem as encountered with the fast one-electron nonaqueous systems.

The colorless two-electron Sn^{II}/Sn^{IV} chloride system was also examined in acetonitrile solution, with n-butylpyridinium salts. Unfortunately, because of extreme irreversibility of these couples [i.e., $SnCl_2/SnCl_4$, $SnCl_3^-/SnCl_5^-$, $SnCl_3^-/SnCl_6^{2-}$, etc.], complicated by the ready reduction of Sn^{II} to Sn°, only very low open circuit voltages, (~0.25 V) were obtained with CdS, CdSe, and GaAs photoanodes. Addition of pyridine or iodide ion to the solution did not improve the results. These redox systems will not be examined further, however, similar couples that are expected to be more reversible may be considered in the future, e.g., $Sn(dtc)_2/Sn(dtc)_2Cl_2$, where dtc = dithiocarbamate.

3.2 Chemical Modification of the Electrode Surface

3.2.1 Electrochemically Generated Polymer Films

In principle, the problem of photoanode degradation could be overcome by the use of an electrically conducting polymer film on the electrode. By acting as a barrier to ion/solvent transport, such an insoluble film could prevent photodegradation while permitting electron exchange with the electrolyte. Good adhesion, uniformity and interfacial charge transport properties can be expected for electrochemically generated films since deposition

is initiated at the interface by electrochemical oxidation/reduction. Electrodeposition of polypyrrole films, having conductivities in the 10 to 100 Ω^{-1} cm^{-1} range, on metal electrodes has recently been reported [28-30]. Under this program, we have photoelectrochemically generated polypyrrole films on semiconductor electrode surfaces and have evaluated the characteristics of the resulting photoanodes [31,32]. Some results generated under our internal IR&D program for n-GaAs and n-Si are included here for comparison.

Experimental Details

Unless otherwise noted, polypyrrole films were electrodeposited from mechanically-stirred acetonitrile solutions containing 0.5-0.1 M pyrrole and 0.2-0.3 M Et_4NBF_4 (supporting electrolyte). The counterelectrode was a 25 cm^2 Pt foil. Deposition on Pt electrodes was performed at a constant potential of +0.85 V vs SCE (saturated calomel electrode). Deposition on n-type semiconductors was performed under tungsten-halogen illumination (100 mW/cm^2) at constant potential (0.45 V vs SCE for n-GaAs, 0.2 V for the Cd chalcogenides, and 0.4 V for n-Si) such that the current, which remained constant except for an initial spike, was in the 2-3 mA/cm^2 range. Based on the charge passed (20 mC/cm^2), the film thickness used was 50-100 monolayers. All electrode potentials are reported vs SCE and measurements were made with iR compensation. Illumination for photoresponse studies was also provided by a tungsten-halogen lamp.

Semiconductors were single crystals (~0.2 cm^2) and were polished using aqueous alumina slurries to 1 μm particle size before mounting in RTV silicone rubber (M-Coat C, M-Line Assessories, Romulus, MI). Crystal orientations were perpendicular to the c-axis for CdS and CdSe, <111> for CdTe, and <111> or <110> (comparable results) for GaAs. Ohmic contacts were made by standard techniques. GaAs electrodes were etched in a 1:1 mixture of concentrated H_2SO_4 and 30% H_2O_2 for about 15 sec (until matte black finish was obtained) prior to use. Si electrodes were etched in 49% aqueous HF solution for 10 seconds. CdSe, CdTe and CdS electrodes were etched in 3 M HNO_3, concentrated HNO_3, and 6 M HCl, respectively. CdSe and CdTe were dipped in a polysulfide solution after etching.

Films on Pt

Electrodeposited polypyrrole films were first prepared (on Pt electrodes) by Diaz et al. [28], who also investigated their electrical and electrochemical properties [28-29]. They found that films deposited from acetonitrile/tetraethylammonium tetrafluoroborate electrolytes are adherent (on metal electrodes) and consist of polymerized pyrrole units plus BF_4^- anions, typically in the ratio of about 4:1 [28]. The films are stable in air to at least 250°C [29] and as electrodes in both aqueous and nonaqueous electrolytes [28-30]. Reversible electrochemical oxidation/reduction of the film is evident from cyclic voltammetry and is associated with a transition from insulating to highly conducting behavior [30]. This film redox process involves exchange of anions between the film and the electrolyte, as evidenced by the dependence of the redox potential on the nature of the electrolyte [30]. Anodic of the transition potential (about -0.2 V vs SCE in both aqueous and acetonitrile solutions), polypyrrole films exhibit electrochemical behavior similar to that observed for Pt electrodes, i.e., solution redox reactions occur reversibly. Data obtained in our laboratory are in general agreement with these results, except that the films appear to slowly decompose with potential cycling in aqueous solutions (containing ferro-ferricyanide) of pH > 13, long-term stability above pH 10 being questionable.

The redox behavior of a polypyrrole film on Pt is shown in Fig. 10. The film is quite stable and can be oxidized and reduced repeatedly with no evidence of peeling or decomposition. The anodic peak currents vary linearly with the sweep rate as expected for a surface bound species, yet the broadness of the cathodic wave and the noncoincidence of the anodic and cathodic peak potentials suggest that there are some kinetic limitations in the electron-transfer process. This presents no problem since the film would normally be operated in the potential region in which the film is conducting, i.e., anodic of -0.2 V. In this case, it is possible to oxidize and reduce electrolyte species through the film. This is illustrated in Fig. 11 which shows a cyclic voltammogram for a polypyrrole-coated Pt electrode in acetonitrile solution containing ferrocene. The observed redox behavior is similar to that obtained for a bare metal electrode.

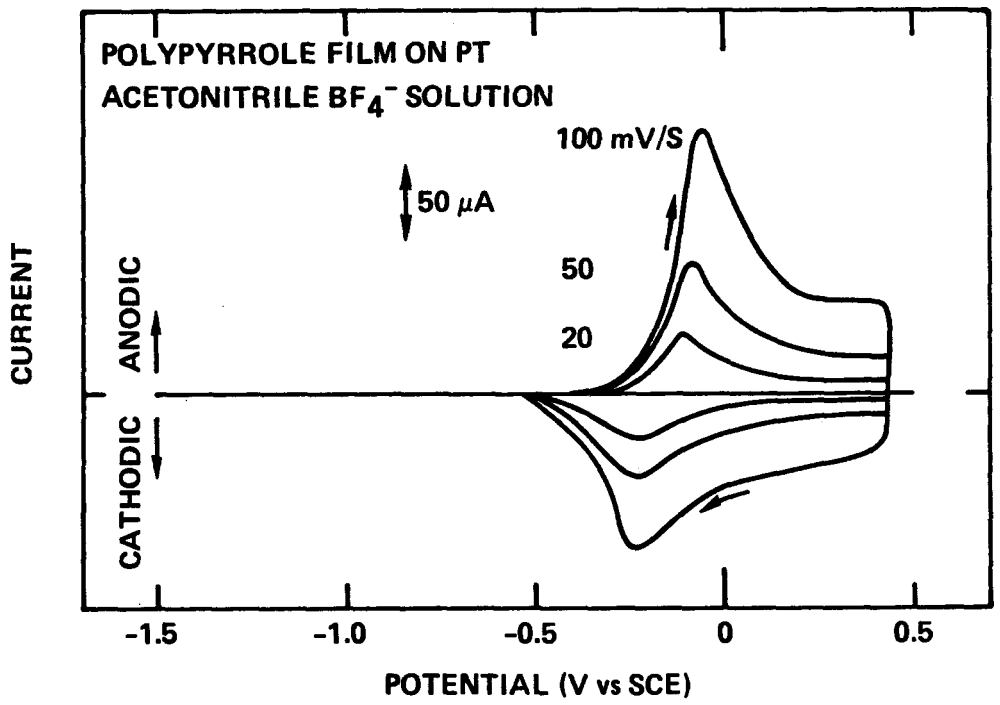

Fig. 10 Cyclic voltammogram for a polypyrrole film on Pt in acetonitrile/0.1 M Et_4NBF_4.

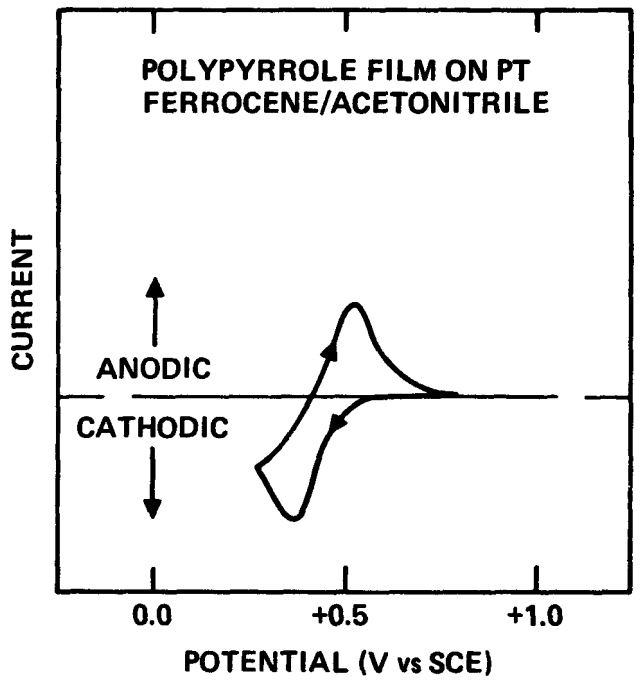

Fig. 11 Cyclic voltammogram at 200 mV/sec for a polypyrrole-coated Pt electrode in acetonitrile/0.1 M Et_4NBF_4/ferrocene solution.

Electroactive species can also be incorporated in the film matrix. For example, polypyrrole films containing $Fe(CN)_6^{3-}$ are produced from acetonitrile electrolytes containing this anion instead of BF_4^-. Cyclic voltammograms for a thin polypyrrole-$Fe(CN)_6^{3-}$ film (on Pt) in an aqueous ferro-ferricyanide solution are shown in Fig. 12. Voltammetry peaks corresponding to the $Fe(CN)_6^{3-/4-}$ redox reaction are evident at about 0.2 V. The linear dependence of the peak heights on sweep rate and the near coincidence of the anodic and cathodic peak potentials are characteristic of a surface-bound redox species. The voltammetric behavior depicted in Fig. 12 was unchanged after more than 50 cycles. Upon transfer of such electrodes to solutions not containing electroactive species, the peaks corresponding to the $Fe(CN)_6^{3-/4-}$ reaction gradually disappear as the redox species is lost to the solution. Likewise, the ferro-ferricyanide reaction on thin polypyrrole films deposited from solutions containing only BF_4^- anions initially exhibits the reversibility characteristic of that observed for Pt (some peak separation) but the anodic and cathodic peaks become more coincidental with potential cycling in the ferro-ferricyanide solution. These results show that electroactive species can be incorporated within polypyrrole films and clearly demonstrate the mobility of anions in the polymer matrix.

Films on Semiconductors

Figure 13 shows linear sweep cyclic voltammograms for a polypyrrole-coated n-GaAs electrode under illumination in an acetonitrile solution containing only supporting electrolyte. The film redox behavior is similar to that observed on Pt (Fig. 10) except that the voltammetry peaks occur at potentials about 0.5 V more cathodic, with the onset for film oxidation corresponding to the semiconductor flatband potential (-1.0 V). As expected, the film redox reaction does not occur on n-GaAs in the dark. It is remarkable, however, that the cathodic peak still occurs when illumination is interrupted after the anodic portion of the cycle. This indicates that electron exchange between the film and the semiconductor valence band occurs in both the anodic and cathodic directions. Similar behavior was observed with polypyrrole-coated CdX photoanodes, except that the voltammetry curves were not as well-defined.

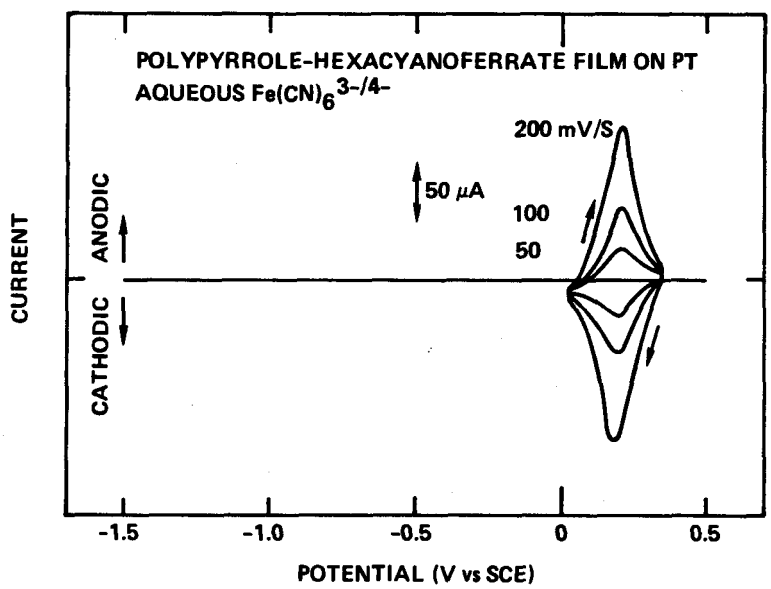

Fig. 12 Cyclic voltammograms at various sweep rates for a polypyrrole-$Fe(CN)_6^{3-}$ film on Pt (~0.1 cm^2) in aqueous 0.1 M $Fe(CN)_6^{3-/4-}$ solution (pH ~ 10).

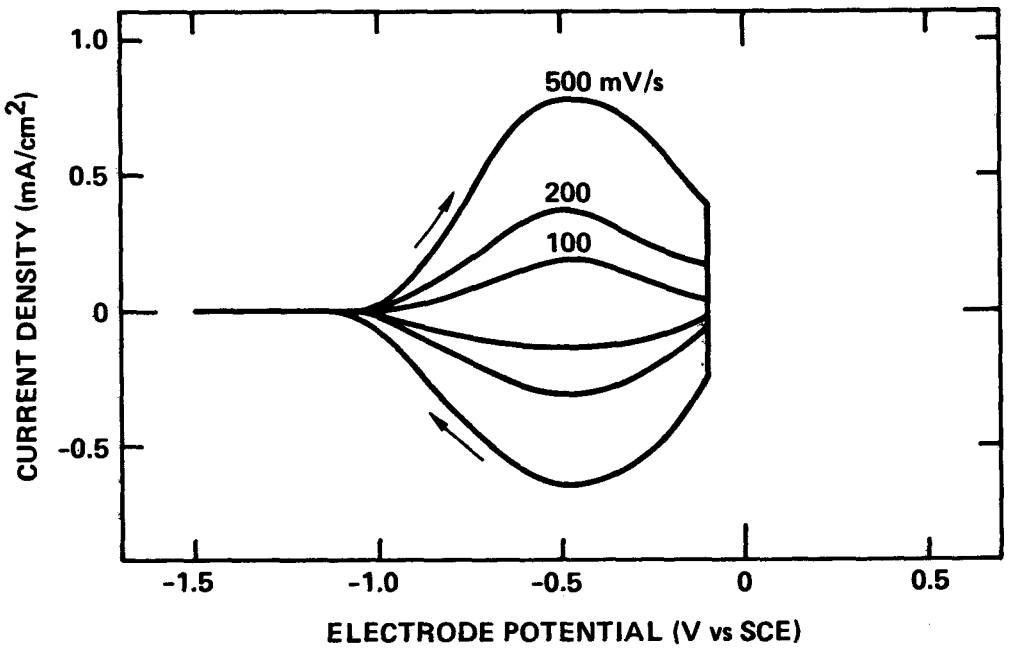

Fig. 13 Cyclic voltammogram for a polypyrrole film on n-GaAs under illumination in acetonitrile/0.1 M Et_4NBF_4.

Photoanode Stabilization

As mentioned previously, polypyrrole films stabilize semiconductor photoanodes against degradation while permitting electron exchange with the electrolyte. This is illustrated for n-GaAs in Fig. 14, n-CdSe in Fig. 15, and n-Si in Fig. 16. In all cases, the short circuit photocurrent for the unprotected (bare) semiconductor decays rapidly (within a few minutes), presumably because of formation of an insoluble blocking surface layer of photodecomposition product, whereas, that for the polypyrrole-coated photoanodes remains practically constant. Note that polypyrrole films also afford n-GaAs electrodes protection from dissolution in aqueous electrolytes, although in this case stabilization is less obvious since the photodecomposition products are typically soluble [33]. At longer times, the film generally peels from the semiconductor surface in toto and the photocurrent decays. This is evident in Fig. 16 for coated n-Si after about 3 minutes. However, in some cases the film remains intact for several days (Fig. 14) and charge equivalent to more than the total weight of the crystal is passed without significant weight loss or degradation of the surface (inspected after film removal). Roughening the semiconductor surface by abrasion prior to film deposition appears to improve the film adhesion.

Peeling problems may be associated with the permeability of polypyrrole films to solvent/solute species, since film stability appears to depend on the nature of the redox couple and/or pH of the electrolyte, and in certain instances semiconductor decomposition underneath polypyrrole films is apparent. For example, polypyrrole-coated n-CdSe photoanodes are stabilized by $Fe(CN)_6^{3-/4-}$ electrolytes (pH = 10-13), but in $Fe^{3+/2+}$ perchlorate solutions (pH = 1), a red layer, presumably Se°, forms within a few minutes under the polymer film (which appears to be intact). These and related observations with a variety of semiconductor materials suggest that polypyrrole films are permeable to solvent/solute species, and that some photodecomposition can occur at the film-semiconductor interface, eventually causing the film to peel. The anion mobility discussed in the preceding section supports this view. Insoluble decomposition products, e.g., hydroxides, Se°, etc., may in some cases collect at the semiconductor-film interface and hinder or slow

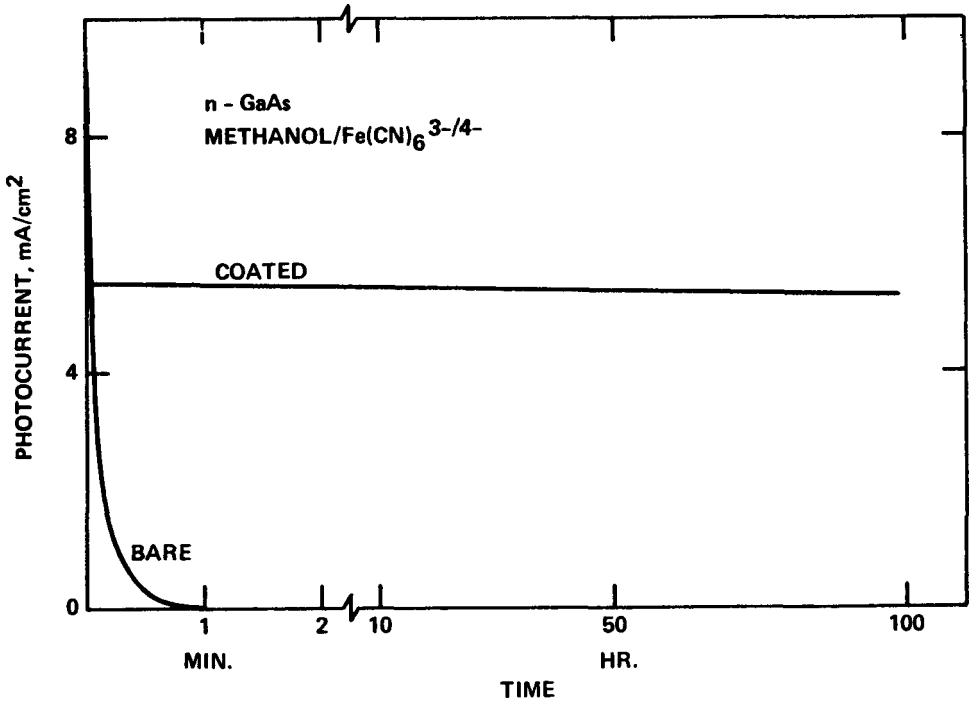

Fig. 14 Short-circuit photocurrent vs time for bare and polypyrrole-coated n-GaAs electrodes in methanol/0.2 M $Fe(CN)_6^{3-/4-}$/0.1 M Et_4NBF_4 solution.

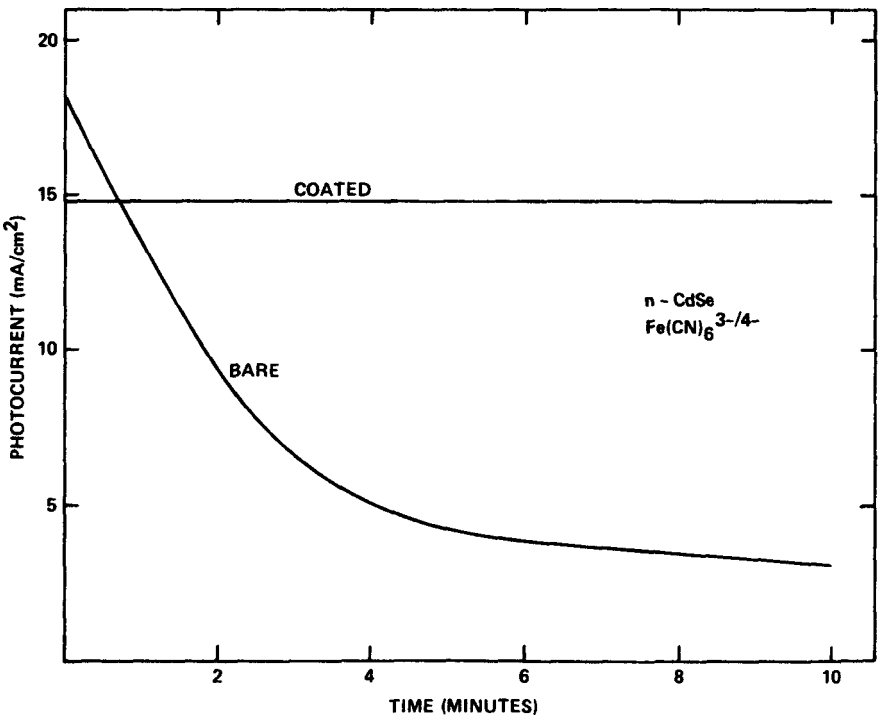

Fig. 15 Short-circuit photocurrent vs time for bare and polypyrrole-$Fe(CN)_6^{3-/4-}$-coated n-CdSe electrodes in aqueous 0.2 M $Fe(CN)_6^{4-}$/0.1 M $Fe(CN)_6^{3-}$ solution (pH ~13).

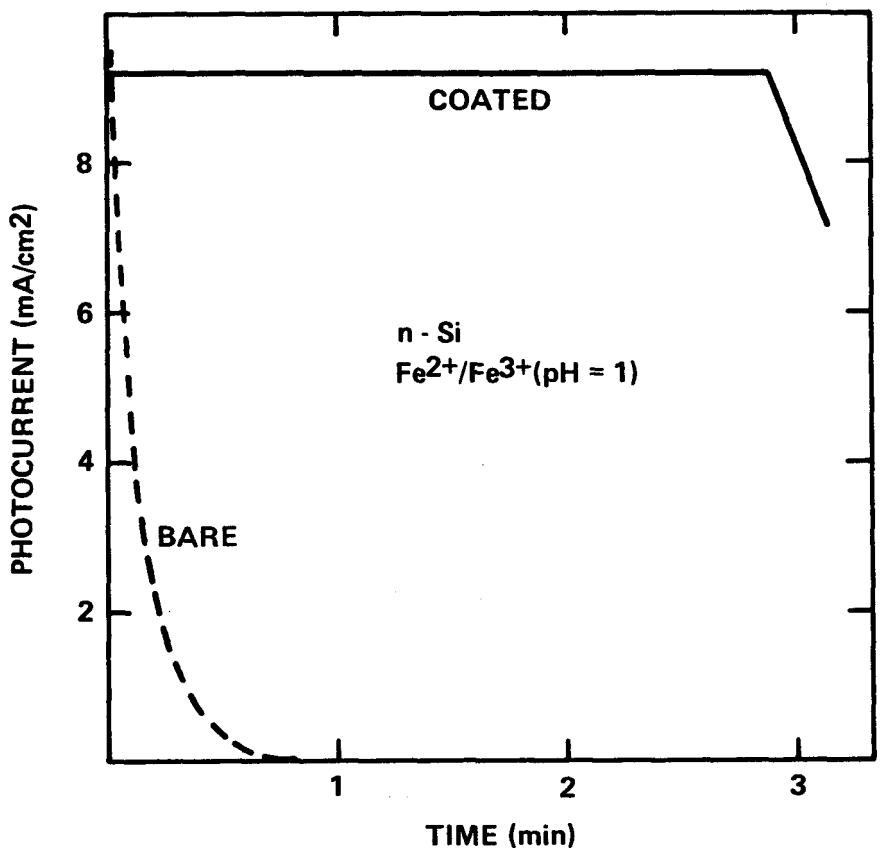

Fig. 16 Short-circuit photocurrent vs time for bare and polypyrrole-coated n-Si in aqueous 0.2 M $Fe(ClO_4)_2$/0.1 M $Fe(ClO_4)_3$/0.1 M $HClO_4$ solution.

further degradation. On the other hand, polypyrrole films have recently been reported to stabilize polycrystalline n-Si in an acidic $Fe^{3+/2+}$ electrolyte [34]. Also, a 5Å Pt film on n-Si has been shown to improve the adhesion of subsequently deposited polypyrrole films [35].

The apparent permeability of polypyrrole films to solvent/solute species poses a serious question regarding the long-term stability of solar conversion devices employing such films. However, it may be possible to circumvent this problem. For example, sufficiently large immobile anions or redox species included in the film during electrodeposition would be expected to significantly reduce the film permeability. Encouragement for this approach is provided by the observed oxidation/reduction of the $Fe(CN)_6^{3-/4-}$ within the polypyrrole film matrix. Although the hexacyanoferrate species was found to be mobile in polypyrrole, there are many larger organic redox species for which this should not be the case. For example, we have deposited conducting polypyrrole films on Pt from acetonitrile/0.01 M Cu(SPc)/0.1 M pyrrole, where SPc is the tetrasulfophthalocyanin tetraanion. The photoelectrochemical properties of such films are currently under investigation. Other approaches are, of course, also possible, including the use of other conducting polymer films or a synergistic combination of film and electrolyte redox couple to provide long-term photoanode stability. Along these lines, we have deposited polyaniline films [36] on various semiconductors (results of these studies are summarized below).

Output Characteristics of Coated Photoanodes

Polypyrrole films apparently do not significantly affect the semiconductor energy levels important in photoelectrochemical processes. Thus, for film-coated electrodes, the flatband potential (V_{fb}) determined by ac impedance or from the photocurrent onset, is practically unchanged, compared to the bare electrode, and remains dependent on the pH of the electrolyte. Also, except for the Cd chalcogenides and Si in acidic ferro-ferricyanide solutions, where appreciable dark currents are observed, the measured open circuit photovoltages (V_{oc}) are generally close to the expected values ($V_R - V_{fb}$), where V_R is the electrolyte redox potential. This is illustrated by the data in Table I, for which V_{fb} values were determined from the photocurrent onset and

Table I. Measured and Calculated Open Circuit Voltages (V_{oc}) for Various Polypyrrole-Coated Photoanodes in Aqueous Solutions.

Semiconductor	Electrolyte*	V_{fb} (V vs SCE)	Calculated V_{oc} ($V_R - V_{fb}$)	Measured V_{oc}
n-GaAs	A	-0.5	1.0	0.95
	B	-0.5	0.8	0.6
	C	-1.1	1.3	1.2
	D	-1.3	1.5	1.37
n-CdTe	A	-0.2	0.7	0.55
	B	-0.2	0.55	0.2
	C	-1.15	1.4	1.2
	D	-1.25	1.5	1.3
n-CdSe	A	-0.1	0.6	0.5
	B	-0.1	0.45	0.1
	C	-0.8	1.0	0.9
	D	-1.1	1.3	1.1
n-CdS	A	-0.4	0.9	0.65
	B	-0.4	0.75	0.3
	C	-0.8	1.0	0.9
	D	-1.3	1.5	1.25
n-Si	A	0.0	0.5	0.4

*Electrolyte A is 0.2 M Fe^{2+}/0.1 M Fe^{3+} perchlorates (pH = 1, V_R = 0.51 V), electrolyte B is 0.2 M $Fe(CN)_6^{4-}$/0.1 M $Fe(CN)_6^{3-}$ (pH = 1, V_R = 0.35 V), electrolyte C is 0.2 M $Fe(CN)_6^{4-}$/0.1 M $Fe(CN)_6^{3-}$ (pH = 13, V_R = 0.22), and electrolyte D is 0.2 M $Fe(CN)_6^{4-}$/0.1 M $Fe(CN)_6^{3-}$/0.1 M CN^- (pH = 13, V_R = 0.22 V).

may not correspond to those measured by ac impedance in all cases. The V_R values, which were measured at a Pt electrode, correspond well with the standard handbook E° values. Note that the V_{oc} values for polymer-coated n-GaAs and n-CdTe in ferro-ferricyanide solution containing excess CN^- are practically equivalent to the bandgap of the respective semiconductors. The increase in V_{oc} produced by excess CN^- can be accounted for by the observed negative shift in V_{fb}, but irreversible photo-oxidation of adsorbed CN^- (e.g., to CNO^-) may also play a role. Since the cell voltage rapidly goes to zero when the electrode illumination is interrupted, the effect of the latter is probably small.

The effect of the polymer film on the photocurrent was difficult to ascertain since results for films produced under ostensibly the same conditions were variable, probably because of the difficulties associated with reproducing the substrate surface and film thickness. The latter was assumed to be directly proportional to the charge passed during deposition which may not be a valid assumption, especially since some semiconductor photodegradation undoubtedly occurs as deposition is initiated. In some cases, the photocurrents for the polymer-coated electrodes approached those for the bare semiconductor but the behavior depicted in Fig. 17 was more typical. In this case, the film is seen to reduce the photocurrent by about 30%. This reduction could be due to light absorption within the film or enhanced charge carrier recombination associated with interface states formed at the semiconductor-film interface. As mentioned previously, the reduction in open circuit voltage (Fig. 17) is apparently due to cathodic dark current introduced by the film, which suggests that interface states may play a role. However, if such effects are not too pronounced, performance characteristics for polypyrrole-coated electrodes could approach those for the bare semiconductor for sufficiently thin films. Of course, a compromise would be required between photoanode stability and performance.

Conducting polypyrrole can also be deposited from aqueous acidic solutions containing pyrrole. For example, in stirred 0.5 M pyrrole solution adjusted to pH 1.5-1.9 with sulfuric acid, polypyrrole deposition is initiated on Pt at +0.65 V vs SCE. We have deposited such films on illuminated n-CdS,

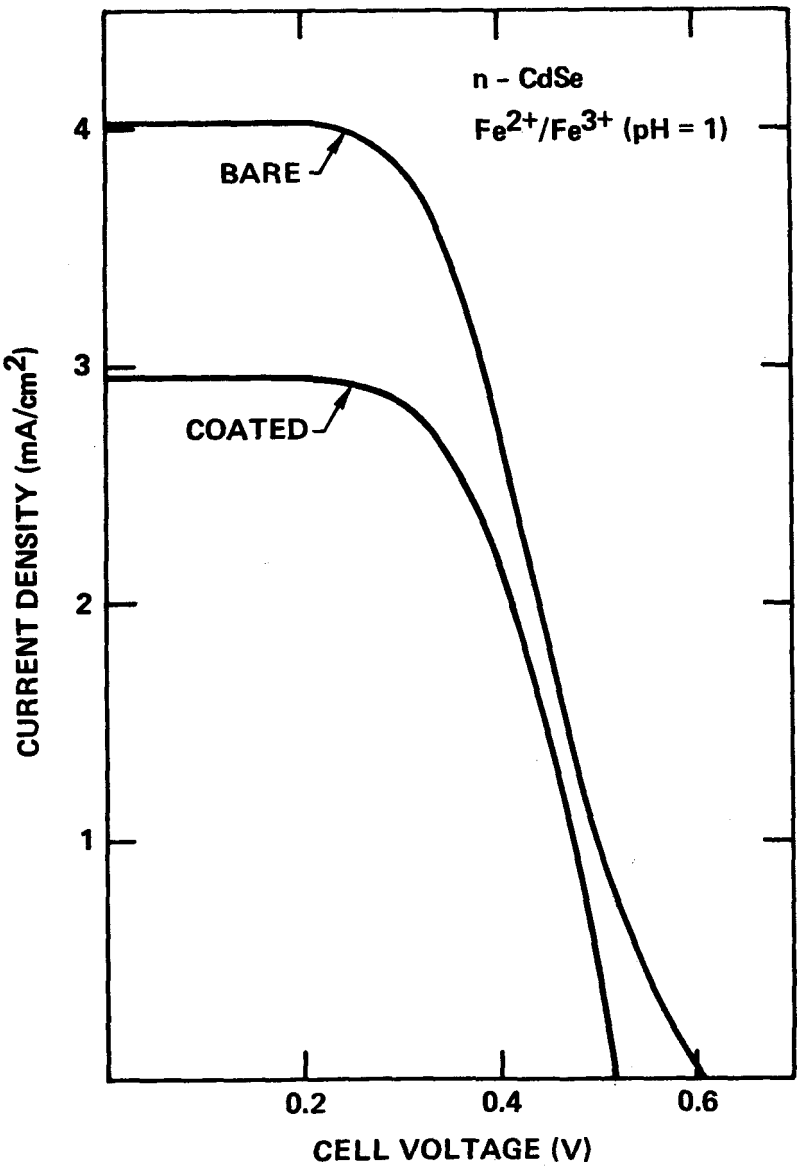

Fig. 17 Photocurrent-voltage curve for bare and polypyrrole-coated n-CdSe in aqueous 0.2 M $Fe(ClO_4)_2$/0.05 M $Fe(ClO_4)_3$/0.1 M $HClO_4$ solution.

n-CdSe, and n-Si electrodes biased at +0.2, 0.0, and +0.6 V, respectively, and obtained results comparable to those for acetonitrile-derived films. By use of these aqueous deposition procedures, anions not readily soluble in nonaqueous solvents can be incorporated in polypyrrole films. Thus, it may be possible to prepare denser, less permeable films by utilizing smaller anions, e.g., Cl^- incorporated from HCl solution. Larger anions, e.g., polystyrenesulfonate incorporated from aqueous polystyrenesulfonic acid solutions (Polysciences, Inc., Warrington, PA) adjusted to pH 1.7 with pyrrole, cannot migrate in and out of the film during oxidation/reduction and may afford films which are more stabilizing for photoanodes.

Polyaniline Films

Another class of conducting polymer film, polyaniline (aniline ≡ aminobenzene) has recently been described by Diaz, et al [36], who deposited this material electrochemically on Pt from aqueous H_2SO_4 solutions containing aniline. Unlike polypyrrole, charge compensation during oxidation/reduction of polyaniline films involves proton elimination/addition and requires an acidic aqueous electrolyte. We have initiated studies of this material and have found polyaniline to deposit adherently on stationary Pt electrodes from 0.2 M aniline in dilute H_2SO_4 (pH 1.7) when the electrode potential is pulsed between +0.8 and -0.2 V at 5 cycles/sec. Addition of N-phenyl-p-phenylenediamine to the electrolyte accelerates the deposition rate markedly. The films remain conducting only in low pH aqueous solutions and are irreversibly deactivated in neutral or basic media. They are also conducting in acetonitrile electrolytes containing ferrocene.

Polyaniline was deposited onto illuminated n-CdS by potential cycling at 50 mV/sec between +0.4 and -0.7 V (SCE) in a static aniline/H_2SO_4 electrolyte. For n-CdSe, the cycle limits were +0.2 and -0.6 V. Although the semiconductor energy levels were not significantly affected by the film, photodecomposition of photoanodes in $Fe^{3+/2+}$ perchlorate solution at pH ~1 was not entirely suppressed. These results are similar to those for polypyrrole covered CdX photoanodes in this electrolyte. Conducting polymer materials containing a mixture of polypyrrole and polyaniline (and possibly some

copolymer) were also deposited on Pt from a static aqeuous H_2SO_4 solution (pH ~1.7) containing equal amounts (~0.2 M) of the monomers by potential pulsing between +0.8 and -0.2 V. The polymer mixture offered no apparent advantage compared to the pure materials. In general, polyaniline and the polymer mixtures did not appear to be as stable as polypyrrole and irreversibly decomposed in neutral and basic media. Polyaniline, which is more conductive in acidic electrolytes, may yield better results with other semiconductor materials that are more stable in acidic media. The behavior of these films in nonaqueous systems also remains to be investigated.

Summary

The results reported here show that electrodeposited polymer films greatly suppress photodegradation of semiconductor photoanodes in some electrolytes while permitting efficient electron exchange with the electrolyte. Performance characteristics attainable with such film-coated photoanodes are typically comparable to those obtained for the bare electrode. Peeling is currently a problem which appears to be associated with permeability of the film to solvent/solute species.

3.2.2 Langmuir Films

Evaluation of the Langmuir technique as a method of applying insoluble organic films to protect CdX photoanodes from degradation was completed. Our previous studies indicated that such thin films were unstable but interpretation of the data was tenuous, since for the film materials investigated it had been necessary to use surfacants to attain wetting of the electrode surface. Recently, we successfully deposited films of barium stearate (which is known to transfer easily to various substrates) onto clean, polished (0.05 μ grit) single crystal n-CdS, as well as some n- and p-GaAs substrates. Such films, up to 7 monolayers, appeared to oxidize under illumination at anodic potentials and immediately peeled from the surfaces of the n-type semiconductors, yet remained stable and insulating on the p-GaAs in aqueous 0.1 M $NaClO_4$ electrolytes. Generation of CO_2 gas by oxidation of the film carboxylate groups could account for this behavior on n-type materials.

Single monolayer films of redox active $n\text{-}C_{16}H_{33}NMe_3^+Ni(mnt)_2^-$, which are not expected to undergo this type of oxidative decomposition, were deposited onto n-CdS and n-GaAs substrates. While no current was observed upon biasing these systems in aqueous $NaClO_4$ electrolytes in the dark, irradiation led to apparent film loss and wetting of the semiconductor surfaces. Considering these formidable problems, Langmuir film deposition was not be pursued further.

3.2.3 Solvent Evaporated Films

Evaluation of the solution evaporation technique for applying insoluble redox-active salt films was also completed. Films of $(C_7H_{15})_4N^+Ni(mnt)_2^-$, which on Pt can be made conducting in aqueous electrolytes, were deposited on stationary and rotating n-CdS (single crystal, polished) electrodes by evaporation of the acetonitrile solvent. Such film-covered electrodes deteriorated rapidly under illumination at anodic potentials in aqueous $Fe(CN)_6^{3-/4-}$ electrolytes. In view of the promising results obtained with electrochemically generated polypyrrole films, the solvent evaporation technique will be abandoned.

3.2.4 Solution Additives

Some additional effort was devoted to investigating charge transfer mediators designed to enhance the partial stabilization of CdS photoanodes by the $Fe(CN)_6^{3-/4-}$ couple in aqueous solution. Phenothiazine, imidazole, 4,4'-bipyridyl, and hydroxide ion were evaluated with polished single crystal n-CdS in 0.1 M each $Fe(CN)_6^{3-/4-}$ solutions containing 0.05 M Na_2SO_4 supporting electrolyte. Under short circuit conditions (0.8 mA/cm^2), an insoluble film (presumably sulfur resulting from lattice decomposition) formed within two minutes in solutions saturated with phenothiazine or 4,4'-bipyridyl (both of which are sparingly soluble), but did not form in solutions containing 0.1 M imidazole or 0.1 M OH^- ion. These latter species also increased the open circuit voltages from 0.7 to 0.9 V. The effectiveness of these additives, compared with 4,4'-bipyridyl and phenothiazine, can be attributed to their greater solubilities which lead to better coverage of the electrode surface, and to favorable shifts in V_{fb}.

While results with imidazole and hydroxide ion as charge transfer mediators were promising, the redox couple was found to be photolytically unstable in aqueous solutions. In sealed glass containers under Ar in the sunlight, aqueous 0.1 M each $Fe(CN)_6^{3-/4-}$ solutions formed colloidal Prussian blue-type precipitates within hours, and this was not prevented by the presence of SO_4^{2-}, I^-, Cl^-, SCN^-, or dodecylsulfate ions. With hydroxide ion (0.2 M and 1.0 M), ferric hydroxide precipitated on the container walls. Solutions containing imidazole turned deep red (no precipitate), indicative of partial photosubstitution for CN^- in the hexacyanoferrate complex. All solutions had an HCN odor and CN^- was detected electrochemically on Pt, also indicating breakdown of the redox species.

3.3 Development of Photocapacitance Spectroscopy

As part of this program, photocapacitance spectroscopy is being evaluated as an in situ method for characterization of PEC photoanodes. In the photocapacitance technique, which to date has been applied extensively only in solid-state studies [37-43], the capacitance of a reverse-biased semiconductor electrode is measured as a function of the wavelength of incident sub-bandgap light. Since the semiconductor space charge capacitance in the dark is generally very small, appreciable changes in the capacitance result from the additional charge introduced by optical population/depopulation of electron/hole traps or surface states. The latter should be distinguishable from bulk states from the effects of species adsorbed from the electrolyte and/or the electrode potential on the photocapacitance spectral features. The density of states can be estimated from the change in the space charge capacitance produced by the incident light.

Our preliminary studies of n-GaAs and n-CdSe electrode in aqueous solutions indicated that peaks occur in the photocapacitance spectra. Work in this area during the past year has been directed toward establishing that such peaks do indeed correspond to processes initiated by sub-bandgap light and upgrading the equipment to permit fully automated measurements to be made over a wide frequency range and at longer wavelengths of light. GaAs was chosen as the model system since most solid-state photocapacitance measurements have

been made on this material. Illumination was provided by a 1000 W tungsten-halogen lamp.

To eliminate the possibility that photocapacitance peaks might be attributable to second-order bandgap light from the monochromator, a wafer of GaAs (~1 mm thick) was used as a filter. Figure 18 shows the capacitance of n-GaAs as a function of the intensity of sub-bandgap light. The observed monotonic increase in electrode capacitance with light intensity established the existence of a detectable sub-bandgap response, but with the equipment then available resolution of the spectral features was difficult.

The upgraded photocapacitance equipment comprises a Solartron Model 1170 Frequency Response Analyzer, a Stonehart Model BC1200 potentiostat, a Hewlett-Packard Model 9825 desk top computer, an Instruments SA Model HT-20 double grating monochromator, and a 1000 W mercury-halogen lamp. With this equipment, the electrode impedance characteristics can be measured as a function of frequency (to 10 kHz) and electrode potential automatically, and light energies to as low as 0.5 eV can be attained.

Preliminary studies indicate that the electrochemical photocapacitance method is extremely sensitive and will ultimately provide valuable new information. A representative photocapacitance spectrum for n-GaAs in aqueous 0.5 $\underline{M}$ K_2SO_4 solution is shown in Fig. 19. Six distinct peaks (at 0.89, 0.98, 1.03, 1.06, 1.14 and 1.25 eV) are evident. Note that measurements at longer wavelengths cannot be made in aqueous solutions which absorb light strongly above 1400 nm. Such spectral features depend strongly on the source of the semiconductor material, the electrode surface pre-treatment, the electrolyte, the prior illumination history of the electrode, the electrode potential, and the measurement frequency. Obviously, considerable additional work will be required to ascertain the nature of such peaks which may arise from optical transitions occurring within the semiconductor, within a surface oxide layer, or at the various interfaces between the semiconductor, electrolyte and oxide.

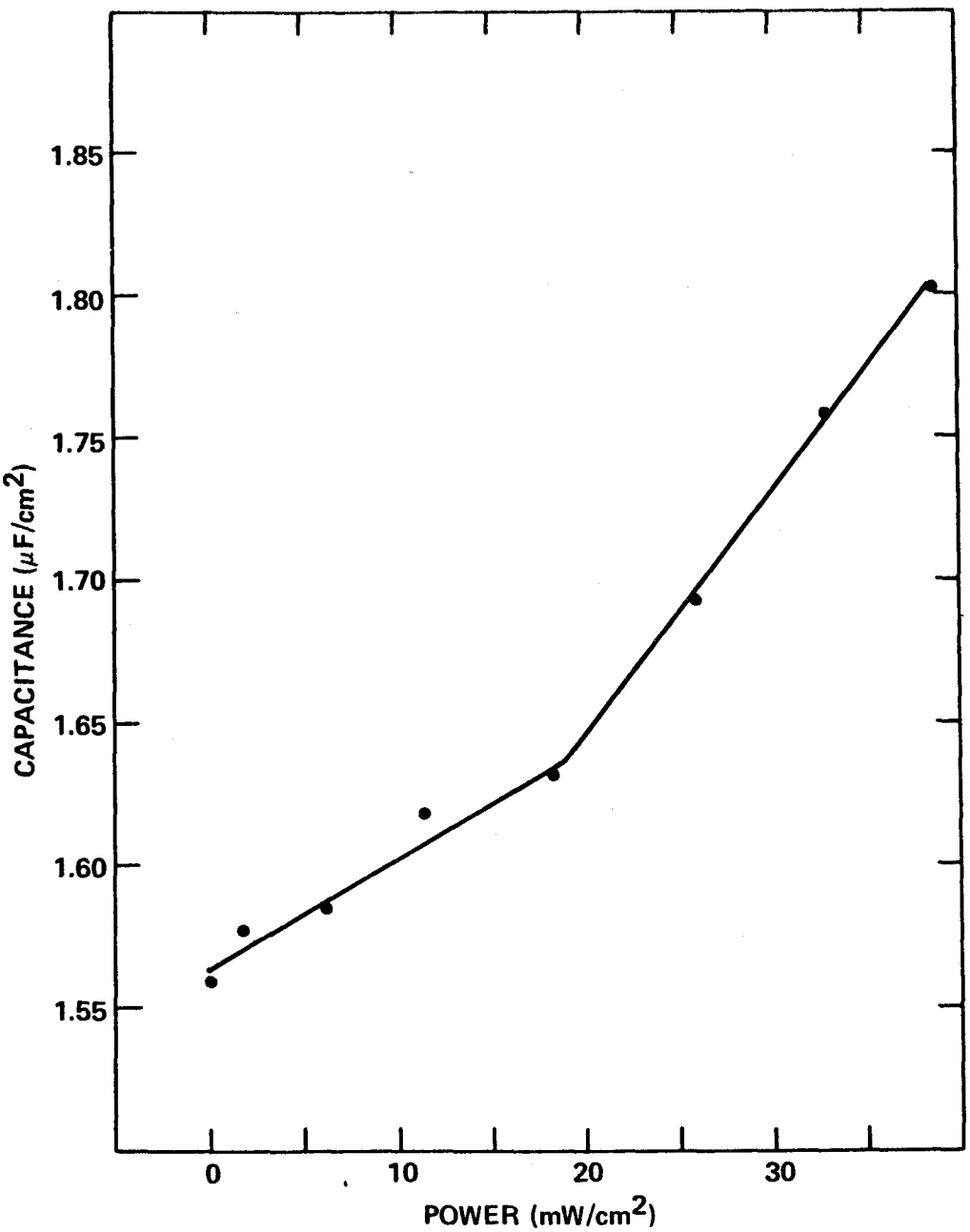

Fig. 18 Capacitance of an n-GaAs electrode (-0.50 V vs SCE) in aqueous polysulfide solution (1 M KOH + 1 M Na_2S + 1 M S) vs intensity of sub-bandgap light of mixed wavelengths.

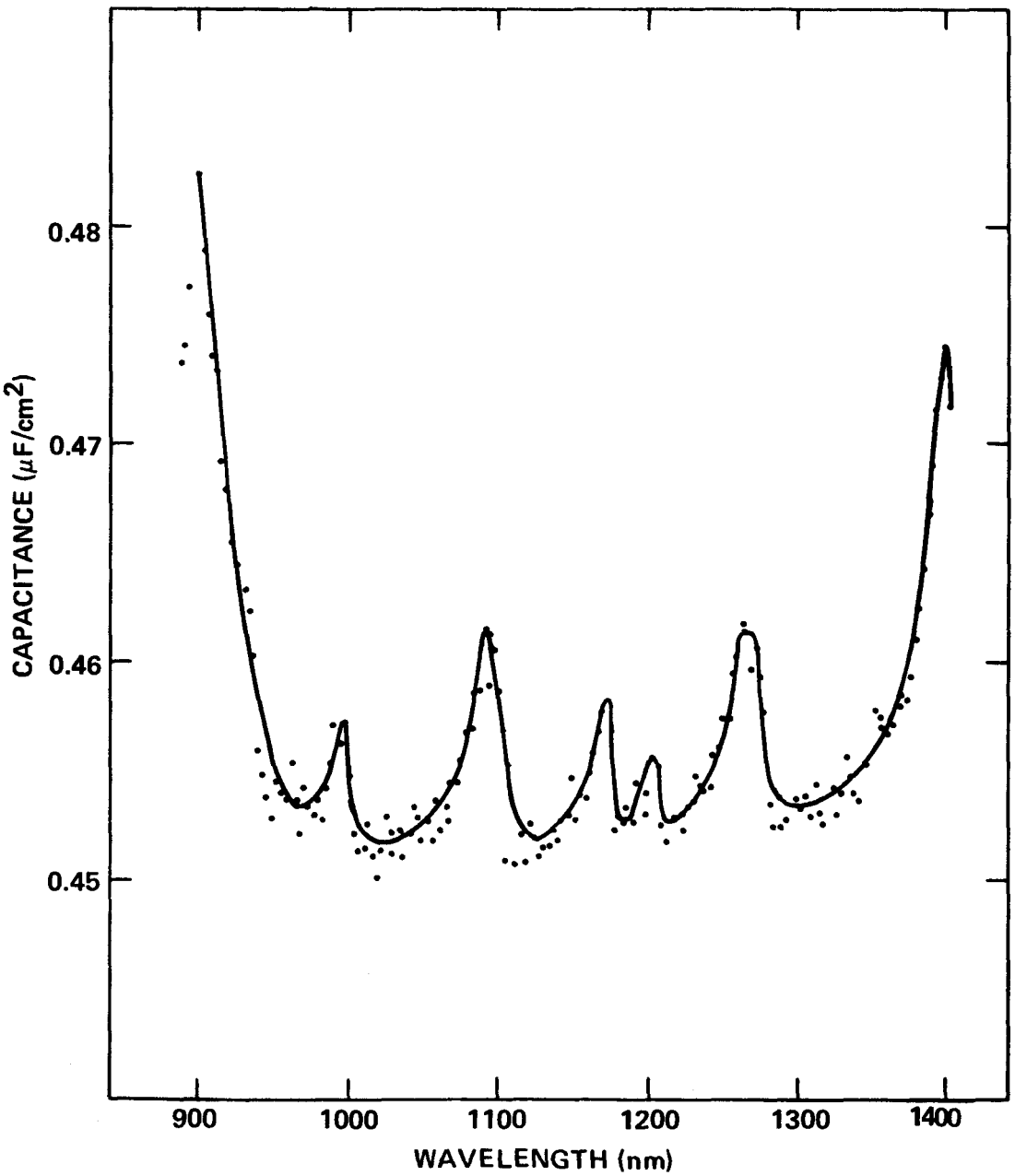

Fig. 19 Photocapacitance spectrum (10 Hz) for an n-GaAs electrode at -0.60 V vs SCE in 0.5 M K_2SO_4 solution.

4.0 REFERENCES

1. R. Noufi, P. Kohl, and A. J. Bard, J. Electrochem. Soc., 125, 375 (1978).

2. A. B. Ellis, S. W. Kaiser, and M. S. Wrighton, J. Am. Chem. Soc. 98, 1635 (1976).

3. A. B. Ellis, S. W. Kaiser, and M. S. Wrighton, ibid., p. 6418.

4. A. B. Ellis, S. W. Kaiser, and M. S. Wrighton, ibid., p. 6855.

5. A. B. Ellis, S. W. Kaiser, J. M. Botts and M. S. Wrighton, ibid., 99, 2839 (1977).

6. G. Hodes, J. Manassen, and D. Cahen, Nature (London), 261, 403 (1976).

7. G. Hodes, D. Cahen, and J. Manassen, ibid., 260, 312 (1976).

8. J. Manassen, G. Hodes, and D. Cahen, J. Electrochem. Soc, 124, 532 (1977).

9. B. Miller and A. Heller, Nature (London), 262, 680 (1976).

10. A. Heller, K. C. Chang, and B. Miller, J. Electrochem. Soc., 124, 697 (1977).

11. T. Inoue, T. Watanabe, A. Fujishima, K. Honda, and K. Kohayakawa, ibid., 124, 719 (1977).

12. H. Minoura, T. Oki, and M. Tsuiki, Chem. Lett., 1279 (1976).

13. Y. G. Chai and W. W. Anderson, Appl. Phys. Lett, 27, 183 (1975).

14. H. Gerischer, J. Electroanal Chem., 58, 263 (1975).

15. H. Gerischer and J. Gobrecht, Ber. Bunsenges. Physik. Chem., 80, 327 (1976).

16. K. C. Chang, A. Heller, B. Schwartz, S. Menezes, and B. Miller, Science, 196, 1097 (1977).

17. R. Noufi, P. Kohl, J. Rogers, Jr., J. White, and A. J. Bard, J. Electrochem. Soc., 126, 949 (1979).

18. D. Cahen, G. Hodes, and J. Manassen, J. Electrochem. Soc., 125, 1623 (1978).

19. A. Heller, J. P. Schwartz, A. G. Vadinsky, S. Menezes, and B. Miller, J. Electrochem. Soc., 125, 1156 (1978).

20. (a) H. Gerischer and J. Gobrecht, Ber. Bunsenges. Phys. Chem., 82, 520 (1978); (b) H. Gerischer and W. Minalt, Electrochim. Acta., 13, 1239 (1968); (c) H. Gerischer, J. Electroanal. Chem., 82, 133 (1977).

21. B. A. Parkinson, A. Heller, and B. Miller, Appl. Phys. Lett., 33, 521 (1978).

22. R. Noufi, D. Tench, and L. F. Warren, J. Electrochem. Soc., 127, 3310 (1980).

23. V. G. Levich, Physicochemical Hydrodynamics, Prentice-Hall, Englewood Cliffs, NJ, 1962.

24. E. Gritzner, K. Danksagmuller and V. Gutman, J. Electroanal. Chem., 72, 177 (1976).

25. F. H. Burstall and R. S. Nyholm, J. Chem. Soc., 3570 (1952).

26. A. A. Schilt, J. Am. Chem. Soc. 82, 3000 (1960)

27. N. S. Gill and F. B. Taylor, Ingor. Synth. 9, 138 (1967); J. L. Ryan, ibid 15, 231 (1974).

28. A. F. Diaz, K. K. Kanazawa and G. P. Gardini, J.C.S. Chem. Comm., 635 (1979).

29. K. K. Kanazawa, A. F. Diaz, R. H. Geiss, W. D. Gill, J. F. Kwak, J. A. Logan, L. F. Rabolt and G. B. Street, J.C.S. Chem. Comm., 854 (1979).

30. A. F. Diaz and J. I. Castillo, J.C.S. Chem. Comm., 397 (1980).

31. R. Noufi, D. Tench and L. F. Warren, J. Electrochem. Soc., 127, 2310 (1980).

32. R. Noufi, D. Tench and L. F. Warren, accepted for publication, J. Electrochem. Soc.

33. H. Gerischer, Ber. Bunsenges., 69, 578 (1965).

34. R. Noufi, A. J. Frank and A. J. Nozik, J. Am. Chem. Soc., 103, 1849 (1981).

35. T. Skotheim (Linköping Institute of Technology, Sweden), private communication.

36. A. F. Diaz and J. A. Logan, J. Electroanal. Chem., 111, 111 (1980).

37. E. Fabre, C. R. Acad. Sc. Paris, 270, 848 (1970).

38. H. Kukimoto, C. H. Henry and F. R. Merritt, Phys. Rev. B, 7, 2486, 2499 (1973).

39. D. Bois, J. Physique, 35, C3-241 (1974).

40. Y. Marfaing, J. Lascaray and R. Triboulet, Inst. Phys. Conf. Ser. No. 22, 201 (1974).

41. K. Sakai and T. Ikoma, Appl. Phys., 5, 165 (1974).

42. A. M. White, P. Porteous and P. J. Dean, J. Electronic Mat., 5, 91 (1976).

43. P. K. Vasudev and R. H. Bube, Solid-State Electronics, 21, 1095 (1978).

☆U.S. GOVERNMENT PRINTING OFFICE: 1981-740-145/2548